**EXELIS**

NIST in Space:
Better Remote Sensors for Better Science
NIAC Phase 1 Final Report
June 26, 2013

Joseph Predina (PI), Exelis Geospatial Systems, Fort Wayne, IN

Dr. Steven Lorentz (Co-I), L-1 Standards & Technology, New Windsor, MD

Acknowledgements

**This work was performed jointly by Exelis Inc., Fort Wayne, Indiana
and L-1 Standards and Technology Inc., New Windsor, Maryland.**

Principle Investigator (PI)
    Mr. Joseph Predina
    Technical Fellow
    Exelis Inc.
    1919 Cook Rd.
    P.O. Box 3700
    Fort Wayne, Indiana 46801
    260-348-5179
    joe.predina@gmail.com

Co-investigator (Co-I)
    Dr. Steven Lorentz
    President
    L-1 Standards and Technology Inc.
    209 High St.
    P.O. Box 729
    New Windsor, Maryland 21776-0729
    410-635-3300
    lorentz@L-1.biz

We also wish to acknowledge the other researchers who contributed to this project

Dr. Allan Smith	L-1 Standards and Technology Inc.
Ms. Kim Slack	Exelis Inc.
Dr. Perry Ramsey	Exelis Inc.
Mr. Wes Gerber	Exelis Inc.

Table of Contents

1. Summary

The objective of this research was to determine feasibility of improving measurement accuracy of space based remote sensors operating in the UV/VIS/NIR bands (250 nm – 3000 nm) by an order of magnitude over technology currently used in space and in electro-optic laboratories throughout the world. Improvements in measurement accuracy are needed to benefit a broad range of science in the field. Specifically, our objective was to devise a practical system architecture that could achieve measurement accuracies comparable to the National Institute of Standards and Technology (NIST) while operating in a space flight environment.

1.1 Why this Is Important

One of the most controversial topics of our day that garners significant public debate is global warming, its root causes, its rate of progression and what should be done about it. Since the economic, environmental and political consequences related to this issue are far-reaching, it is important to have accurate scientific data to better understand what is happening to our planet and in order to make well informed political choices in response. The small changes associated with the Earth, sun and space energy balance that drive global warming occur on top of an enormous daily energy exchange. This is just one example that illustrates the importance of precise scientific measurements.

Remote sensors operating in space provide the best vantage point for monitoring the energy balance between Earth, space and the sun which ultimately impacts climate on our planet. Historically, use of weather satellite data archives to establish long term climate trends has been difficult and filled with controversy since these existing space assets were not designed for this purpose. Limitations related to spectral resolution, spectral range observed, radiometric accuracy, long term stability and calibration differences between various sensors made it difficult to use satellite data to develop undisputable climate records for trending the earth energy balance over time. Today's fielded technology is not adequate to meet the need and there are no plans in place to launch sensors accurate enough to make these measurements over the next decade through 2022.

The inadequacy of space-based remote sensor technology is rooted in the fundamental difficulty of measuring the quantity of spectrally resolved earth reflected solar energy (irradiance, radiance) to accuracies better than the current standard of ~2% over decade-long space missions. What's needed in order to develop reliable climate trending records of the earth energy balance are space based remote sensor systems that achieve better than 0.1% measurement accuracies over decade-long missions where these measurements are tied directly to undisputed international standards.

It is surprising to find in this age of sophisticated technology (smart phones, HDTV, supercomputers, space exploration, astronomy, etc.) that it is still difficult to measure accurately something so fundamental as the quantity (power) of spectrally resolved light. To date, only the most sophisticated national laboratories such as NIST can achieve spectrally resolved <0.1% measurement accuracies in the solar bands by using very sophisticated equipment combined with labor intensive and tedious processes that span many days to achieve calibration on a single spectrometer.

Earth observing space-based remote sensors needed to support climate trending will require re-calibration on timescales of minutes, operation in a hostile environment and very simple hardware implementations that achieve the desired 0.1% measurement uncertainties. We believe that the "NIST in Space" concept as described in this report achieves these objectives and lays the groundwork for future proof of concept through prototype demonstrations.

Moreover, other applications covering a broad range of NASA science missions not related to climate change can benefit. Commercialization of the concept for use in electro-optic laboratories worldwide is also foreseen. Any scientific application requiring precision photon flux measurements in the 250 – 3000 nm wavelength range will benefit.

1.2 What is NIST in Space?

We call our concept "NIST in Space" because it will enable space based remote sensors to measure the quantity of light (irradiance, radiance) in the solar bands more accurately than ever before. The objective is to replicate the low radiance measurement uncertainty associated with the National Institute of Standards and Technology (NIST) and then to tie these remote sensor measurements to an undisputed Standard International (SI) scale. In so doing, we also overcome prior obstacles in replicating National Laboratory grade calibration in the space environment for decade long missions.

This objective is met through the unique combination of components depicted in Figure 1-1:

1) Un-cooled broadband Active Cavity Radiometer (ACR)

2) Multi-color light emitting diode (LED) integrating sphere source

3) White light source & black target

4) UV/VIS/NIR Fourier Transform Spectrometer (FTS)
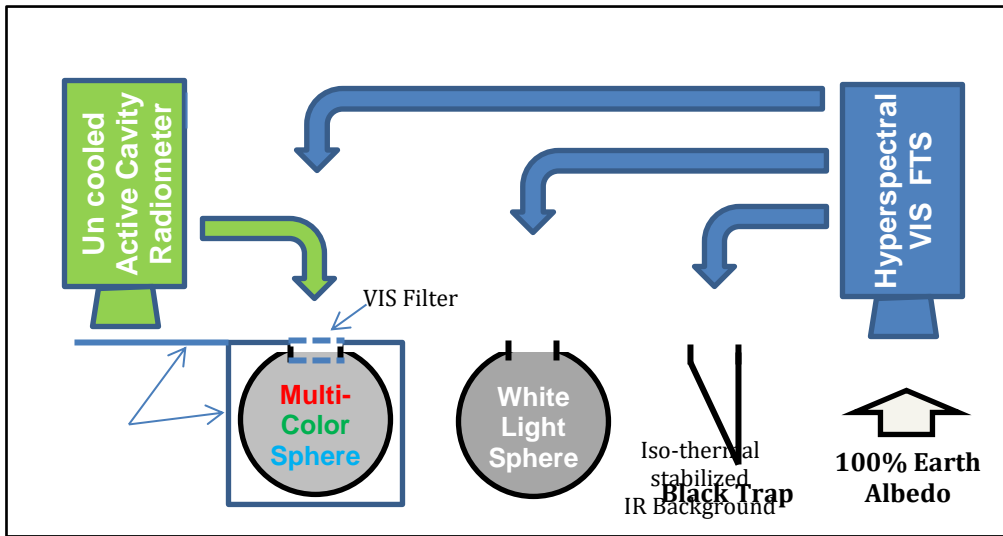
Figure 1-1: NIST in Space Concept (250 – 3000 nm)

The multi-band hyperspectral UV/VIS/NIR Fourier Transform Spectrometer (FTS) instrument is the primary earth viewing remote sensor as depicted in Figure 1-1. This instrument spectrally resolves earth scenes viewed into thousands of independent spectral channels over the solar wavelength range 250 nm to 3000 nm. The choice of FTS architecture over the more commonly used grating or prism spectrometer is an important distinction for the NIST-in-Space concept. The FTS instrument architecture has special unique properties that make NIST-in-Space possible. These same properties are not found in grating or prism spectrometer architectures as will be discussed later.

The FTS is periodically re-calibrated on-orbit using a conventional two point calibration process involving a white light source and black target. For purposes of the NIST-in-Space system, the white light source is not a precise calibration reference. It only needs to produce a somewhat continuous emission spectrum from 250 nm to 3000 nm while maintaining a short term stability of 0.1% for only 10 minutes. Long term stability of the white light source is not important and it is permitted to degrade and change emission characteristics significantly over the life of the space mission. The white light source needs no special ground calibration nor does it need any NIST traceability.

The multicolor integrating sphere in Figure 1-1 that uses Light Emitting Diode (LED) sources combines with an un-cooled active cavity radiometer (ACR) to become an on-orbit, International Radiance Standard (SI) at discrete wavelengths spanning 250 nm to 3000 nm. This source is then used to track and correct degradations of the primary white light calibration source carried on the satellite. When combined with the FTS, this suite of flight hardware becomes a generic, highly accurate (~0.1%), spectrally resolved UV/VIS/NIR space based remote sensor. More details are provided later in this report.

1.3 Phase 1 Research Plan

Our NIAC Phase 1 research plan mitigated the highest technological risks associated with the "NIST in Space" concept as listed below. The work breakdown structure also included task management and reporting. All six of the Phase 1 research activities were executed between September 10, 2012 and May 31, 2013.

1. Define the requirements for and model the output of an ACR that can achieve a 0.1% calibration without requiring cryogenic cooling

2. Define the requirements for and model the output of an ACR that can achieve 0.1% calibration for low radiance levels associated with 100% earth albedo

3. Define the requirements for and model the output of the various calibration sources using available space qualified parts: LEDs, fiber optics, lamps, and interfaces

4. Define the requirements for and model the behavior of the thermal system required to stabilize the thermal condition over the measurement period required by the ACR

5. Combine all analysis and models into an implementable system concept that takes NIST in Space from TRL2 to TRL3

6. Task management, reporting, presentations & travel to two NIAC symposiums

1.4 Conclusions from Phase 1 Study

The technical risks identified in Section 1.3 were addressed and we can now strongly assert that an order of magnitude improvement in the calibration accuracy of remote sensors operating over the UV/VIS/NIR wavelength range is feasible by using the NIST-in-Space architecture. More specifically, our findings at the conclusion of this Phase 1 study are summarized as follows:

1. The 0.1% calibration uncertainty objective is feasible for measuring the total integrated earth reflected solar radiance relative to a 100% earth albedo radiance in a 10 km field of view footprint on the earth surface from a satellite in a 600 km low earth orbit (LEO) using the NIST in Space concept.

2. A Fourier transform spectrometer (FTS) must be used as part of the NIST-in-Space architecture. Grating or prism spectrometers were found to be incompatible with the concept. An FTS operating from 250 to 3000 nm is an advanced technology yet to be developed since no such device has ever flown in space.

3. It is feasible to house all components of the NIST in Space remote sensor in a volume corresponding to a 6U Cubesat (10 cm x 20 cm x 30 cm). Availability of a larger volume can improve performance in areas of remote sensor stray light control and also to help accommodate a more advance laser driven plasma white light calibration source.

4. Cryogenic cooling of the ACR is not needed to meet the NIST in Space objectives for earth observation. The un-cooled ACR studied in this project that ties the FTS measurements to an international standard is expected to achieve a measurement uncertainty of less than 5 nanowatt when operating at a nominal spacecraft temperature of 300 K. In order to accomplish this measurement uncertainty on-orbit, the change in temperature gradient on the internal surfaces of the ACR structure will need to be less than 500 μK over 10 minute time intervals. The ACR measurement process also cancels the effect of linear changes of ACR bulk temperature that are much larger than 500 μK. These levels of thermal stability are possible using current technology in a closed system that has active thermal control combined with thermal isolation.

5. Cryogenic cooling of the multicolor LED reference integrating sphere is not needed to meet NIST in Space objectives. The broadband ACR may view an un-cooled 300 Kelvin integrating sphere and experience less than 3 nanowatt measurement uncertainty after applying background subtraction techniques. This holds true so long as the integrating sphere temperature changes linearly in time to within 25 millikelvin over 10 minutes. Only the back surface of the sphere viewed by the ACR instrument is required to have this thermal stability. This level of thermal stability is achievable using conventional thermal control techniques. In addition, the sphere will not require a thermally controlled window at its output aperture that was contemplated when this project began.

6. In the near future, an un-cooled ACR and LED integrating sphere Cubesat experiment should be attempted. We believe a 3U Cubesat (10 x 10 x 30 cm) can be used to demonstrate 5 nanoWatt measurement uncertainty over all orbit positions even while undergoing worst case eclipse thermal changes. Thermal simulations conducted under this Phase 1 study show moderate temperature changes of the low mass Cubesat structure making such a future experiment a promising endeavor to pursue in order to further raise the Technology Readiness Level (TRL) of NIST-in-Space.

7. A multitude of LEDs exist with wavelengths spanning the 250 – 3000 nm range that can be space qualified. LED power levels sufficient to enable the NIST in Space concept fall in the range of 100 mW – 500 mW. Multiple LEDs can be combined easily for each desired wavelength to achieve the power level needed.

8. A commercially available broadband laser driven plasma light source is the most desirable technology for use as the white light source used to calibrate the NIST in Space spectrometer. This plasma source produces the flattest spectral emission over the UV/VIS/NIR range. This technology is available commercially and has successfully operated in the lab (TRL4). Adaptation for aerospace systems including spaceflight would be required. This adaptation is believed to only entail standard engineering practice. Plasma source lifetime can range from 15,000 hr – 50,000 hr

thus making possible 10 year space missions if this calibration source is cycled ON and OFF and used only when needed.

9. Five enabling technologies were identified during our Phase 1 study that should make UV/VIS/NIR FTS remote sensors feasible for aerospace systems.

10. A 1 milliG vibration robust FTS remote sensor spanning 250 to 3000 nm wavelength range is believed feasible with recent technology advances. This FTS would have 2.5 cm aperture, 1º FOV and 0.7 cm^{-1} wavenumber resolution. Technology readiness is currently estimated at TRL2 with good chance of advancement to TRL4 through further research and prototype demonstration in the lab.

11. During this Phase 1 study, all of the technical risks identified in Section 1.3 were examined with positive outcomes. We believe this raises the NIST-in-Space concept from TRL 2 to TRL3.

12. Follow-on research should focus on prototype builds of some of the key subsystems.

    a. Cubesat demonstration of the 0.1% measurement accuracy using ACR with LED sphere

    b. Conversion of plasma white light source into an aerospace subsystem

    c. Prototype of 1 milliG vibration robust UV/VIS/NIR FTS remote sensor (250 nm – 3000 nm spectral range, 0.7 cm^{-1} resolution, 1deg FOV, 2.5 cm aperture)

    d. Instrument of Opportunity experiment hosted on the Space Station for the entire NIST-in-Space remote sensor concept with all subsystems integrated together

2. Better Remote Sensors for Better Science

2.1 Climate Change & Earth Energy Balance

Satellite sensors are most useful in measuring and trending the earth radiation balance as illustrated in Figure 2-1. However, since changes in the incoming, reflected and emitted radiation are small in comparison to the enormous magnitude of radiation exchanged between the Earth, space and sun, the absolute accuracy achieved by remote sensors in making these measurements becomes paramount.

Note that Figure 2-1 shows a net energy flux imbalance of 0.9 W/m² as the forcing which was driving climate change as estimated in 2010. Compare that number to 341.3 W/m² solar irradiance estimated as the earth daily average (day, night, all solar angles) or to the 1365.2 W/m² solar irradiance at top of earth atmosphere at high noon. One can conclude that accurately measuring the 0.9 W/m² imbalance requires all measurements of incoming and outgoing radiation to be much better than this (i.e. three times better). For solar measurements, that would equate to ~0.1 % measurement accuracy relative to the earth daily average.
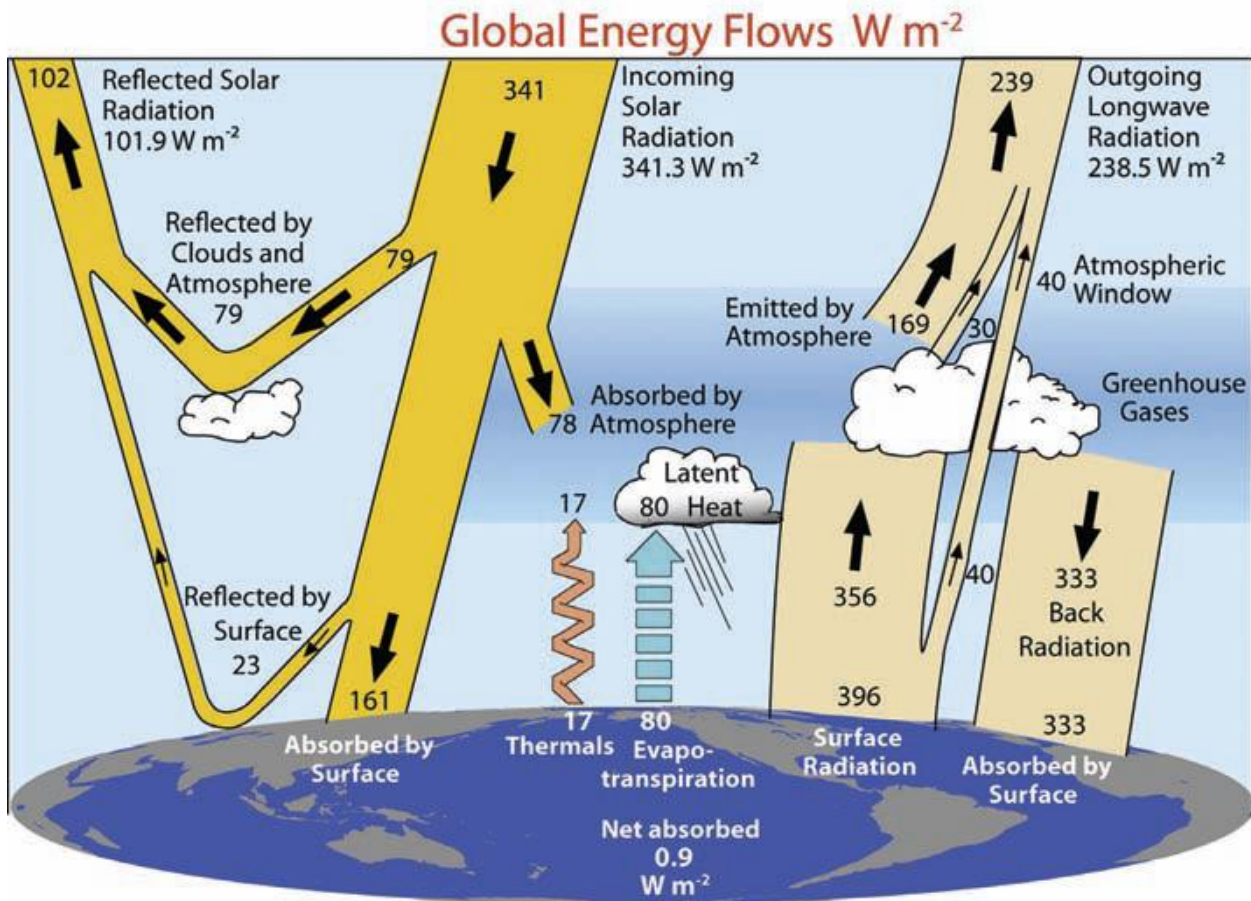
**Figure 2-1: Typical radiation balance between earth, sun and space averaged over 24 hours
(source: Trenberth 2010)**

The uncertainty associated with the various elements of the model in Figure 2-1 is still quite high in comparison to the 0.9 W/m² estimated to be absorbed by the earth. The International Panel on Climate Change (IPCC) published findings in 2007 that summarized the various human driven factors contributing

to the warming of our planet. These are summarized in Figure 2-2. Greenhouse gases and ozone are the primary warming factors while clouds, aerosols and surface albedo the primary cooling factors. Note that the net anthropogenic forcing as estimated in 2007 was 1.6 W/m^2 with an uncertainty that placed the number anywhere in the range of 0.6 W/m^2 to 2.4 W/m^2. It is interesting to note that most of the uncertainty associated with estimating the earth energy balance is associated with reflection of solar radiation tied to surface albedo, aerosols and clouds. Furthermore, the magnitude of the uncertainty associated with the total net anthropogenic radiative forcing illustrated in Figure 2-2 (1.8 W/m^2 peak-to-peak) is comparable to the magnitude of the bias estimated (1.6 W/m^2). Thus, climate models have a large uncertainty in their radiative forcing estimates and satellite remote sensors with unprecedented measurement accuracy are needed to help resolve this.
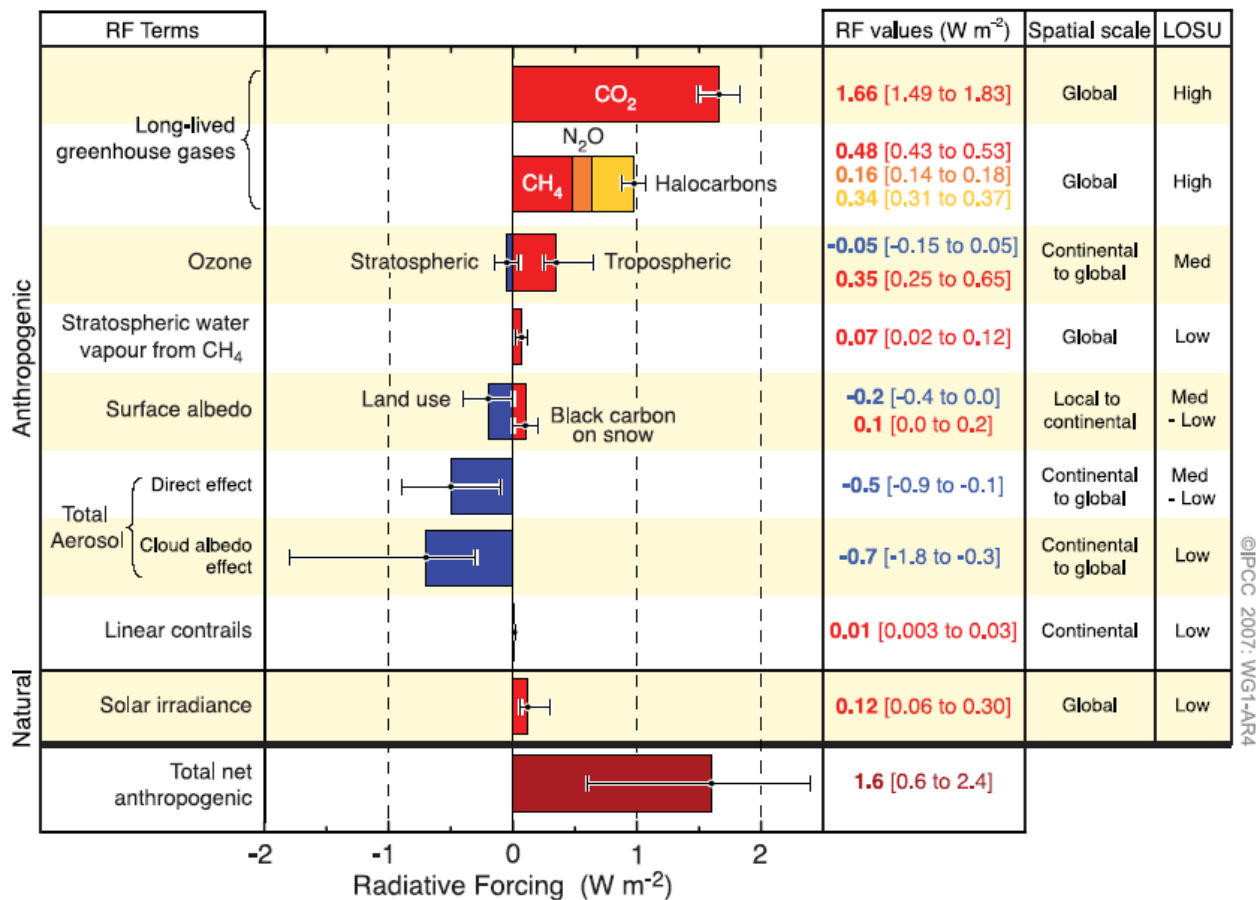
Figure 2-2: Anthropogenic radiative forcings contributing to global warming/cooling (IPCC 2007)

2.2 Remote Sensors that Meet Science Needs

The measurement accuracy needed to perform undisputable climate trending from space has undergone refinement over time with the most significant consensus reached in 2002 when scientists from NASA, NOAA, NIST, NPOESS-IPO and various universities published their findings (Table 2-1) as part of the Climate Change Research Initiative. These recommendations assumed that the remote sensor stability per decade should be at least 5 times smaller than the expected change of climate parameter trended. The recommendations have not undergone significant change since originally introduced in 2002.

**Table 2.1: Accuracy & Stability Needed from Space Based Remote Sensors
to Trend Climate Change (from Climate Change Research Initiative, 2002)**

	Climate Parameter Trended	Remote Sensor Type	Accuracy	Stability (per decade)
Solar Influences & Clouds	Solar irradiance	Radiometer	1.5 W/m^2	0.3W/m^2
	Surface albedo	Vis radiometer	5%	1%
	Net solar radiation at top-of-atmosphere (TOA)	Broad band solar	1 W/m^2	0.3 W/m^2
	Outgoing long-wave radiation at TOA	Broad band IR	1 W/m^2	0.2 W/m^2
	Cloud base height	Vis/IR radiometer	1 K	0.2 K
	Cloud cover (fraction of sky covered)	Vis/IR radiometer	-	-
	Cloud effective particle size	Vis/IR radiometer	@ 3.7 µm: water 5%, ice 10% @ 1.6 µm: water 2.5%, ice 5%	@ 3.7 µm: water 1%, ice 2% @ 1.6 µm: water 0.5%, ice 1%
	Cloud liquid water path	Microwave	0.3 K	0.1 K
		Vis/IR radiometer	Vis/IR: see cloud optical thickness & cloud top height	Vis/IR: see cloud optical thickness & cloud top height
	Cloud top height	IR radiometer	1 K	0.2 K
	Cloud optical thickness	Vis radiometer	5%	1%
	Spectrally resolved thermal radiance	IR spectroradiometer	0.1 K	0.04 K
	Downward long-wave flux at earth surface	IR spectrometer & Vis/IR radiometer	See tropospheric temperature, water vapor, cloud base height & cover	See tropospheric temperature, water vapor, cloud base height & cover
	Downward short-wave radiation at earth surface	Broad band solar & Vis/IR radiometer	See net solar radiation: TOA, cloud particle effective size, cloud optical depth, cloud top height & water vapor,	See net solar radiation: TOA, cloud particle effective size, cloud optical depth, cloud top height & water vapor,
Atmospheric Influences	*Temperature*			
	Troposphere	Microwave or IR radiometer	0.5 K	0.04 K
	Stratosphere	Microwave or IR radiometer	1 K	0.08 K
	Water vapor	Microwave	1.0 K	0.08 K
		IR radiometer	1.0 K	0.03 K
	Ozone			
	Total column (λ independent)	UV/VIS spectrometer	2%	0.20%
	Total column (λ dependent)	UV/VIS spectrometer	1%	0.20%
	Stratosphere	UV/VIS spectrometer	3%	0.60%
	Troposphere	UV/VIS spectrometer	3%	0.10%
	Carbon dioxide	IR radiometer or DIAL	3%	Forcing 1% Sources/sinks: 0.25%
	Aerosols	VIS polarimeter	Radiometric: 3% Polarimetric: 0.5%	Radiometric: 1.5% Polarimetric: 0.25%
Surface	Ocean color	VIS radiometer	5%	1%
	Sea surface temperature	IR radiometer	0.1 K	0.01 K
		MW radiometer	0.03 K	0.01 K
	Sea ice area	VIS radiometer	12%	10%
	Snow cover	VIS radiometer	12%	10%
	Vegetation	VIS radiometer	2%	0.80%

These recommendations are forcing new ways of thinking when designing satellite sensors for the purpose of trending climate. Since the energy exchange between sun, earth and space spans ultraviolet to the far infrared (0.2 µm - 100 µm), the observations from space must also produce a continuous spectrum over this same range to validate scientific models. The spectral resolution achieved must be fine enough to enable development of better spectroscopic atmospheric models and to improve the knowledge of earth surface properties. New hardware architectures, calibration methods and associated ground processing are required to support the accurate parameter measurements dictated by Table 2-1.

For example, radiance observations in the visible spectrum must be calibrated approximately 10 times more accurately than current methods. Brightness temperature uncertainty for radiometers must approach current NIST characterization limits of 0.01 - 0.03 Kelvin in the infrared bands and maintain this level of calibration for at least 10 years while on-orbit. Spectral calibration and high spectral resolution of radiance observations will be essential in identifying changes in the concentration of trace gas species such as greenhouse gases. Finally, trending of earth cloud fraction, aerosol content and surface vegetation characteristics will be vitally important to future climate models.

The biggest technical challenges come in the solar bands (250 nm – 3000 nm) that currently carry the largest climate model uncertainties and which also have the poorest remote sensor measurement accuracies relative to what is needed.

2.3 Stability or Accuracy?

There is this dilemma associated with information appearing in Table 2-1. Climate scientists really want remote sensors that have measurement uncertainties associated with the far right column of Table 2-1. However, this column is designated as the "stability" of the remote sensor's measurement over one decade of operation in space. The second column from the right designates the remote sensor absolute measurement accuracy and these tolerances are much looser. Realizing the practical limitations of remote sensor technology in 2002, the panelists in their wisdom designated realistic measurement accuracies for these systems.

The gap between these two columns (accuracy versus stability) is bridged by building remote sensors that have much better long term stability as compared to their measurement accuracy. Successive instruments in a series are then launched so that their on-orbit operation overlaps and so that this period of simultaneous operation can be used to remove bias offsets between sensors. The result is a trending record without discontinuities. Attempts are also made to improve the remote sensor absolute measurement accuracy with vicarious calibration techniques that fit remote sensor observations to well-known and well characterized earth scenes.

Figure 2-3 illustrates how this was done for the variety of space based remote sensors used to measure the total solar irradiance between 1978 and 2010. One can see the natural variability of the solar irradiance for 11 year periods due to sunspot number as well as the measurement offsets from one remote sensor to the next due to differences in measurement accuracy.

Figure 2-4 is the result of splicing together these various measurements and removing biases between instruments as reported at the 2008 AGU conference. At that time, a solar constant of 1365.4 W/m^2 had been estimated based upon 33 years of on-orbit trending and based upon adjustments of remote sensor measurements to remove biases. Consequently, discontinuities in the record were removed in this process, but that did not resolve the absolute accuracy of the trended record. Only recently with the launch of the Total Irradiance Monitor (TIM) on the SORCE satellite, subsequent confirmation of these measurements

from the PREMOS instrument and laboratory experiments uncovering measurement errors associated with the prior generation of remote sensors, we now know that the more accurate estimate of solar constant is 1360.8 W/m² (Kopp et al, 2011) as depicted in Figures 2-5 and 2-6.
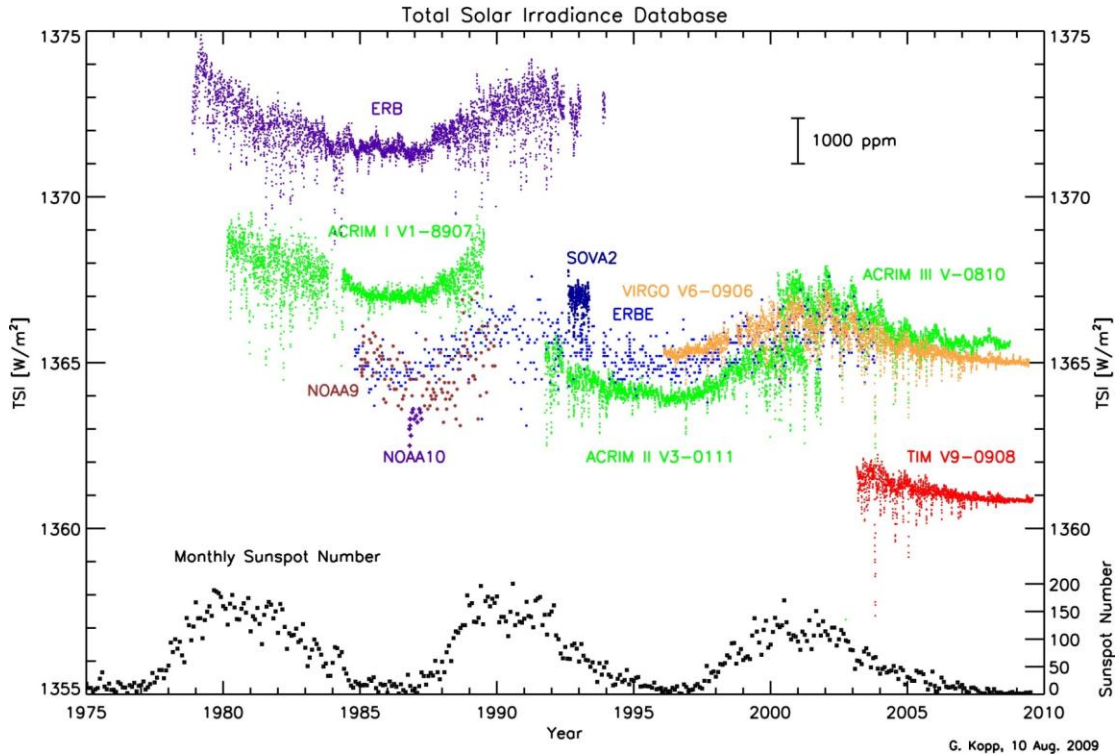
Figure 2-3 Solar irradiance record from 1978 to 2010 as reported by various remote sensors
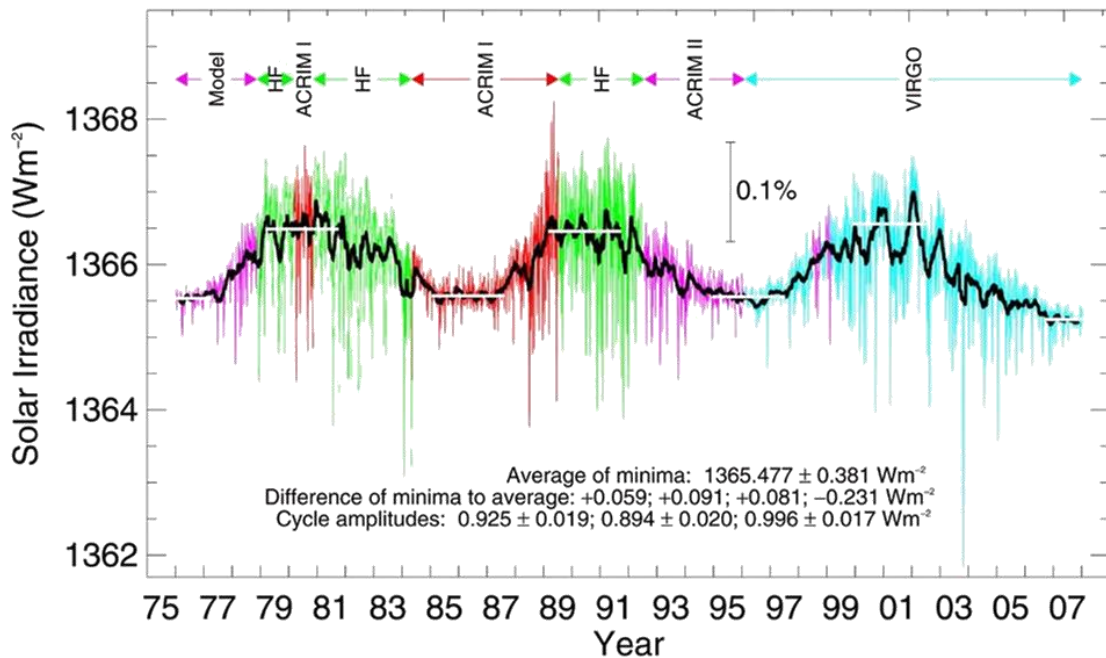
Figure 2-4 Composite solar irradiance record from 1978 to 2010 reported at 2008 AGU conference
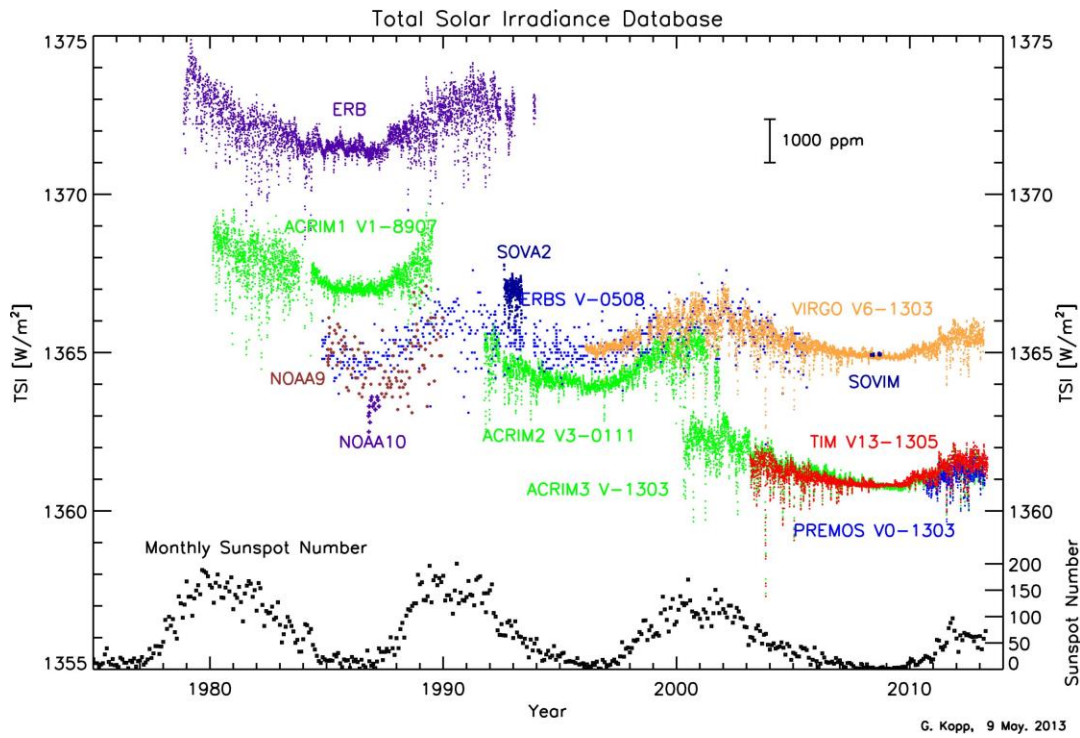
Figure 2-5 Update of solar irradiance record from 1978 to 2013 (G. Kopp, 2013)
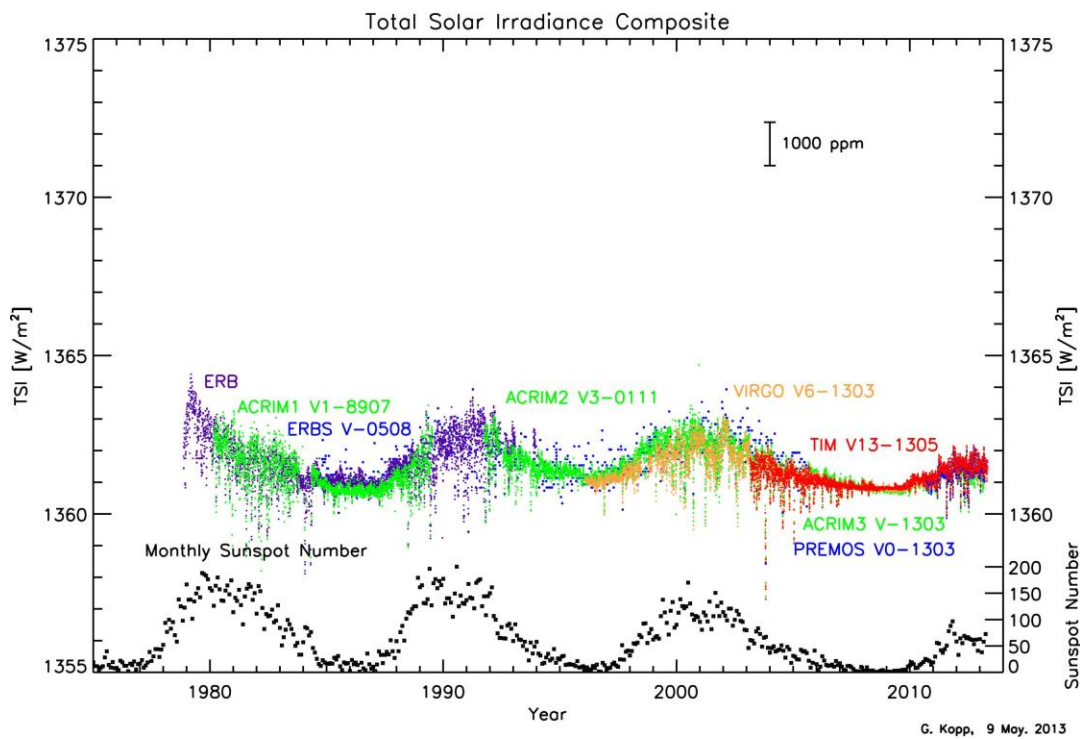
Figure 2-6 Latest composite solar irradiance record after bias removal (G. Kopp, 2013)

The difference between Figures 2-4 and 2-6 is a 4.7 W/m^2 discrepancy in solar constant. After accounting for night/day and solar angle averaging over the entire planet this measurement error converts to a -1.2 W/m2 radiative forcing for purposes of climate models; a number which by itself is comparable to the net anthropomorphic bias estimates in Figures 2-1 and 2-2 that are believed to drive climate change.

All of this illustrates the importance of measurement accuracy over simply relying on measurement stability. It also brings into question the strategy of launching remote sensors into space where science is forced to depend upon stability of remote sensors per Table 2-1 instead of developing the technology needed to improve measurement accuracy of remote sensors.

2.4 Dynamic Range & Spectral Response

The problem is compounded when needing to accurately measure the earth's solar reflected radiance which is a much more challenging than measuring the sun's output. The earth's reflected solar radiance varies significantly on a temporal, spatial and spectral scale across the globe. Figure 2-7 illustrates the type of variation to be expected and also how much smaller the earth radiance is relative to the sun.
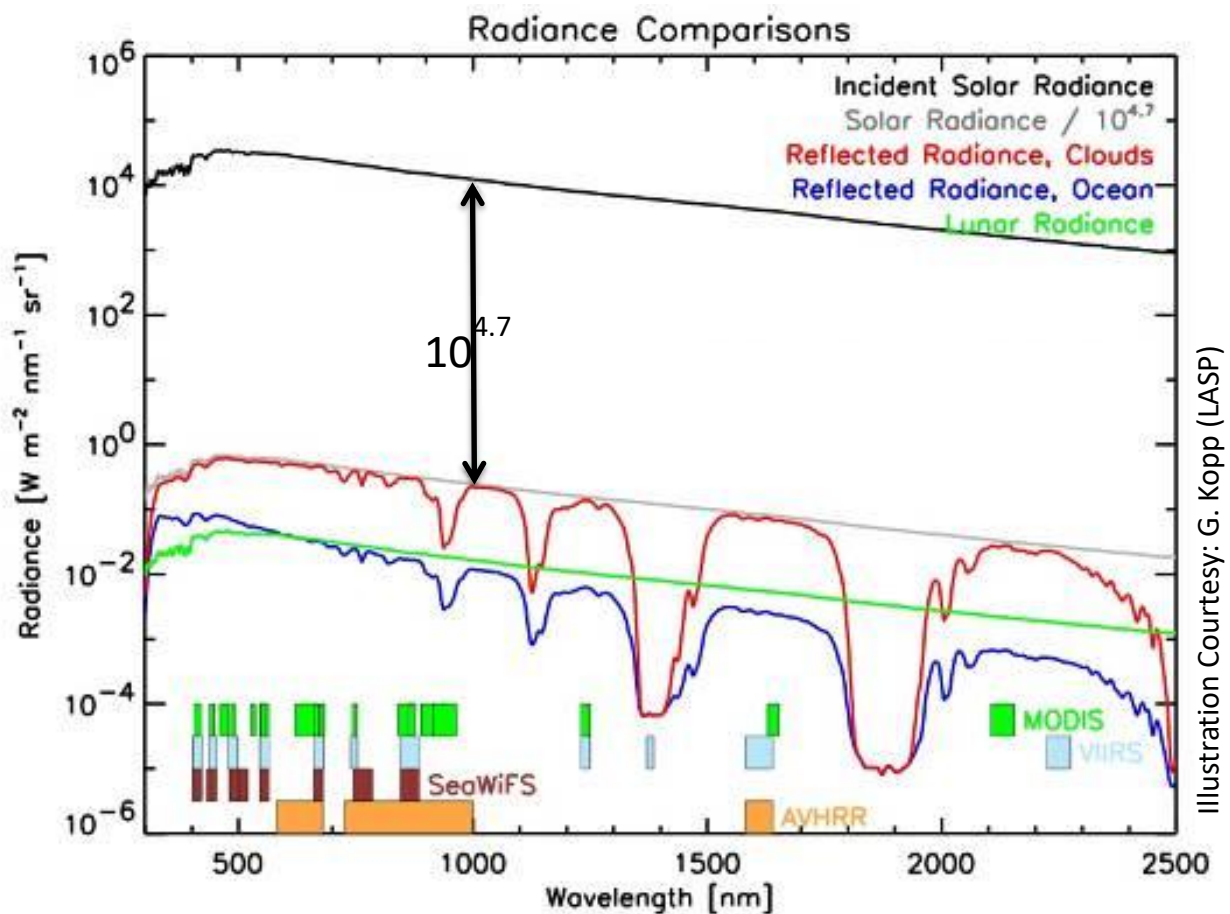
Figure 2-7: Solar radiance and earth reflected radiance differ enormously and measuring both of these accurately is very difficult (Illustration courtesy G. Kopp, LASP)

Broadband radiometers can be used to measure total solar output and earth reflected solar radiance. These types of instruments were identified in many applications called out in Table 2-1. However, very little is learned for purposes of climate trending by using broadband radiometers. In order to identify the mechanisms responsible for changes in the earth energy balance, it is important to measure the spectral distribution of power radiated. Only in this way can cause and effect be traced. Measurements need to be both accurate and spectrally resolved.

Lastly, the sensor dynamic range must span 8 to 9 decades as Figure 2-7 illustrates. Of this, nearly 5 decades of measurement range are needed due to solar and earth radiance differences while another three decades of dynamic range are needed to produce 0.1% measurement resolution/accuracy.

2.5 Potential Impact to Earth Science Measurements

In order to achieve planned mission objectives, future earth science and climate trending instruments require more stringent radiometric accuracy and long term stability performance. Spectrometers spanning the full 0.2 µm – 100 µm wavelength range must monitor the sun, earth and space energy exchanges. The following NASA missions illustrate some of the scientific needs for higher accuracy and improved stability instruments:

GEO-CAPE – Geostationary Coastal and Air Pollution Events (GEO-CAPE) represents the current trend of using panchromatic-hyperspectral-imaging sensors for atmospheric chemistry study and earth surface characterization. Two UV/VIS/NIR FTS sensors are baselined by NASA JPL in the current concept of this Tier III decadal survey mission. The 0.1% calibration capability of our NIST-in-Space concept would enable accurate ocean color measurements for trending eco systems, carbon sinks and for determining atmospheric chemistry processes.

PACE – The Pre-Aerosol, Cloud and ocean Ecosystem (PACE) is a Tier II decadal survey mission. The PACE instrument targets the visible spectral range 360 - 755 nm, with 5 - 15 nm spectral resolution and a signal-to-noise >1500 to resolve the ocean color spectrum associated with plant life concentrations near shorelines. Trending the ecosystem is very important in developing better climate models and in understanding the carbon cycle. Currently, the PACE instrument architecture baselines a 26 channel filter radiometer. However, the precise spectral line shape delivered by a VIS FTS instrument combined with 0.1% calibration would enable a more stable trending of ocean color as compared to a filter radiometer using a solar reference.

Earth Radiation Balance Monitoring – The Climate Absolute Radiance and Refractivity Observatory (CLARREO) was intended to trend the spectrally resolved earth radiation balance from 0.2 µm - 50 µm in order to study forcing and feedback mechanisms associated with climate change. The 2007 International Panel on Climate Change (IPCC) estimates that the total solar irradiance input and reflected output from the earth between 0.2 µm – 5.0 µm must be resolved with a stability of 0.3 W/m^2/decade to accurately trend climate change. When averaged over the entire earth surface, this equates to 0.2% absolute calibration uncertainty per decade in the solar bands. These levels of uncertainty are needed to build better climate models that allow scientists to better understand the forcing and feedback mechanisms that drive global warming.

As of this writing, CLARREO is one of NASA's decadal missions that was delayed due to NASA funding limitations and there are no current plans to launch a system prior to 2022. CLARREO would use a well calibrated infrared FTS instrument for quantifying the earth's thermal emissions and a suite of grating spectrometers to process the solar bands. The same grating spectrometer measures both the solar output

and reflected earth radiance (per Figure 2-7). This is achieved by using a combination of attenuation techniques when observing the sun. In this approach, the Sun is used as a reference for calibration purposes and therefore there is no direct tie to SI. Ratio of the solar measurement and reflected earth measurements yields the average earth albedo that is trended over time.

The NIST-in-Space architecture can enhance the CLARREO objectives by providing spectrally resolved 250 to 3000 nm measurements that are tied to International Standards and which meet the measurement accuracy needed in the solar bands to trend climate over the long term.

3. Enabling Technologies for 0.1% UV/VIS/NIR Calibration in Space

3.1 Prior UV/VIS/NIR Calibration Methods Are Inadequate

The problem with using integrating spheres and light bulbs as calibrators in space is that the optical output of a tungsten bulb/sphere degrades as the bulb is used. The reflective material inside the integrating sphere also becomes contaminated and darkens with time.

As a result, vicarious calibration methods have been used to supplement the calibration process. These methods rely on specific earth landmarks, the moon, direct solar irradiance, inter-satellite comparison or well instrumented ground truth sites. To date, these vicarious calibration methods have had limited impact on calibration uncertainty reaching accuracies of only 2% – 3%. Historically, these vicarious calibration methods have inadequate accuracy for purposes of climate trending as reported by the IPCC in 2007.

An alternate and more popular calibration reference is the solar PTFE diffuser plate (Spectralon) which is used to reflect natural sunlight into the instrument aperture. Unfortunately, the surface of a diffuser plate also degrades over time in a space environment. Solar irradiance also changes with distance of the earth from the Sun, solar sunspot activity and other natural short-term variation of the solar irradiance. This method of calibration typically produces an accuracy of only 0.7% -2% over the long term [22, 23, 24, 25, 26, 27]. Solar diffuser calibration methods are inherently complex from an operational standpoint and require special attention to diffuser illumination angles and an extensive characterization of the solar diffuser material prior to launch.

The moon has also been used as a visible calibration standard when 2%-3% accuracy is sufficient.[19,20] Currently, there is no traceability to SI standards using celestial objects. Attempts have been made to calibrate the ROLO model (USGS) and Vega, traceable to SI standards, but no scales have been produced. Calibrations involving use of the moon are complex and require careful attention to illumination angles, phase of the moon, position of the satellite and occasionally require spacecraft maneuvers to acquire lunar scenes. Lunar calibration is excellent for the purpose of precision, however, with a lack of a SI unit traceable radiance scale, it is not appropriate for absolute calibration

The Total Irradiance Monitor (TIM) and the Spectral Irradiance Monitor (SIM) that fly on the Solar Radiation and Climate Experiment (SORCE) satellite[29] use electrical substitution radiometers for calibration. The TIM measures total solar irradiance with 0.035% accuracy[29], but is not spectrally resolved and does not view the low earth radiance levels. The SIM makes spectrally resolved measurements of the sun with 2% calibration accuracy[29]. Neither of these predecessor instruments can achieve the absolute accuracy and spectral resolution that the "NIST in Space" calibration concept is expected to provide for earth measurements.

3.2 NIST Capabilities

The National Institute of Standards and Technology (NIST) has developed a ground based laboratory solution for obtaining better than 0.01% radiance calibration accuracy over the visible spectral range and 0.05% over the near IR. It is called the Spectral Irradiance and Radiance Responsivity Calibrations using Uniform Sources (SIRCUS) facility[21]. Only in the past decade have these expensive facilities been developed and used by NIST.

SIRCUS requires use of a cryogenically cooled active cavity radiometer (ACR) and cryogenically cooled laser illuminated integrating sphere in order to minimize errors introduced from background infrared emission.

The output of a laser illuminated integrating sphere is detected by an ACR which is the most accurate method known to date for measuring optical power. Once calibrated, the laser source can then be used to calibrate another instrument such as a spectrometer at the same wavelength. The process is repeated for other wavelengths using many tunable lasers from 0.2 to 5 µm wavelength.

The tunable lasers are of various technologies that are incompatible with operation in space. In addition, the size, mass, laser technology type, 20 Kelvin cryo-cooled ACR, and cryo-cooled integrating sphere all preclude any practical use of the existing NIST technology in space. Other equipment includes a 1 meter diameter sphere, ACR II, 2 kW tunable lasers, ultrasonic water bath fiber optic modulator for laser despeckling, 1000 lb optical bench, and as such, must be confined to the laboratory (TRL 4).

3.3 Un-cooled ACR Technology

Our un-cooled ACR technology was invented by Co-Investigator, Dr. Steven Lorentz of L-1 Systems and Technology who previously developed ACR instruments used at NIST. Dr. Lorentz's company also constructs under contract the portable NIST SIRCUS facilities (see Section 3.2) used by various labs throughout the world. He recently developed an un-cooled ACR called NISTAR aboard the DISCVR (Triana) mission. NISTAR is an extraordinarily sensitive and accurate ACR already operating successfully at temperatures above ambient (38°C), has been fully flight qualified and is ready for flight (TRL 8). Figure 3-1 is a photo of this four channel radiometer with thermal shields removed. The ACR contains no optics, only a trap black body, two accurately sized apertures that define the Field of View (FOV) and a shutter mechanism. This ACR has exhibited 10 nW equivalent optical noise detection threshold while operating un-cooled. This level of sensitivity is consistent with the current goal of monitoring 100% earth albedo radiance with 0.1% accuracy as will be discussed later.
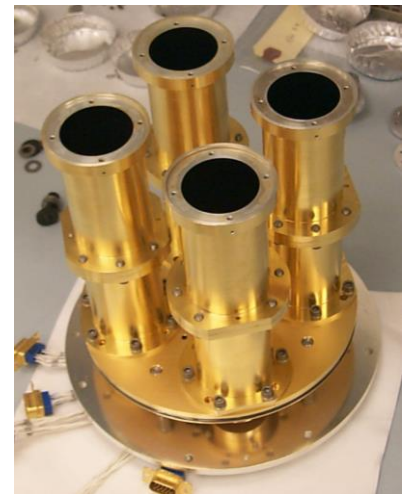
Fig. 3-1: NISTAR Radiometer

In previous generations of this ACR technology[33] the high detection sensitivity to optical power was enabled by a unique thermistor made from polycrystalline barium strontium titanate with dopants added to make it a semiconductor. A sharp rise in the resistance with increasing temperature occurs above the 38°C Curie temperature associated with this ferroelectric phase transition. This results in 1000 Ω/K sensitivity for the trap black body that captures photon energy from scenes being viewed. Thus, the technology incorporated into this NISTAR heritage design makes feasible 0.1% calibration accuracy for an input UV/VIS/NIR optical power of 10 µW.

Unlike NISTAR which uses the ACR to view either deep space or the earth from L-1 orbit, the ACR developed for our "NIST in Space" concept measures the radiance emitted from an un-cooled integrating sphere. As such, the infrared background will be significantly higher than what was encountered with NISTAR. The ACR sensitivity to this varying thermal background, the changing spacecraft temperature and quality of background cancelling techniques to suppress background generated errors is a major challenge in our application.

3.3.1 ACR Concept for NIST-in-Space

A plan is presented to implement electrical substitution radiometry for an ACR in order to measure the radiance of an LED illuminated integrating sphere that acts as a calibration source for the NIST-in-Space

hyperspectral FTS. The basic measurement of the ACR is optical power. Radiance of the source is then inferred given the throughput of a snout fitted with precision apertures that defines the cone of light from the LED illuminated integrating sphere captured by the ACR cavity. The power radiated from the sphere into the ACR is approximately 10 µW and must be measured with an uncertainty of 10 nW (0.1 %) or less. Building such an ACR is feasible, and with careful design, thermal drifts due to orbit-induced spacecraft temperature variations can be mitigated so they do not limit ACR performance.

.Most importantly, the un-cooled ACR which is used as our primary calibration standard has no optical components nor does it have any electronic detectors that can degrade over time. Hence, its calibration accuracy is long lasting and suitable for decade long missions in space without significant change.

3.3.2 ACR Operating Principle

The ACR is a thermal detector consisting of a cone-shaped absorbing receiver that is thermally coupled to a heat sink, see left panel of Figure 3-2. The effective absorptance of the black painted receiver is very high (typically greater than 0.9995) so that nearly all light entering the cavity is converted to heat. The amount of optical heating is deduced by precisely monitoring the power applied to an electrical heater that is used to keep the cavity at constant temperature. When the heat sink is also controlled to constant temperature, then changes in power delivered to the cavity heater correspond to opposing changes in optical power absorbed by the cavity. This technique is insensitive to thermometer calibration, slow changes in the thermal link impedance and contamination of the cavity. A summary of the design characteristics of the ACR considered here is provided in the right panel of Figure 3-2.

ACR Characteristics

Noise floor	5 nW
Type B absolute uncertainty	<0.1 %
Settling time to 0.1 %	<100 S
Field-of-view	4.4°
Defining aperture diameter	4 mm
Snout aperture diameter	5 mm
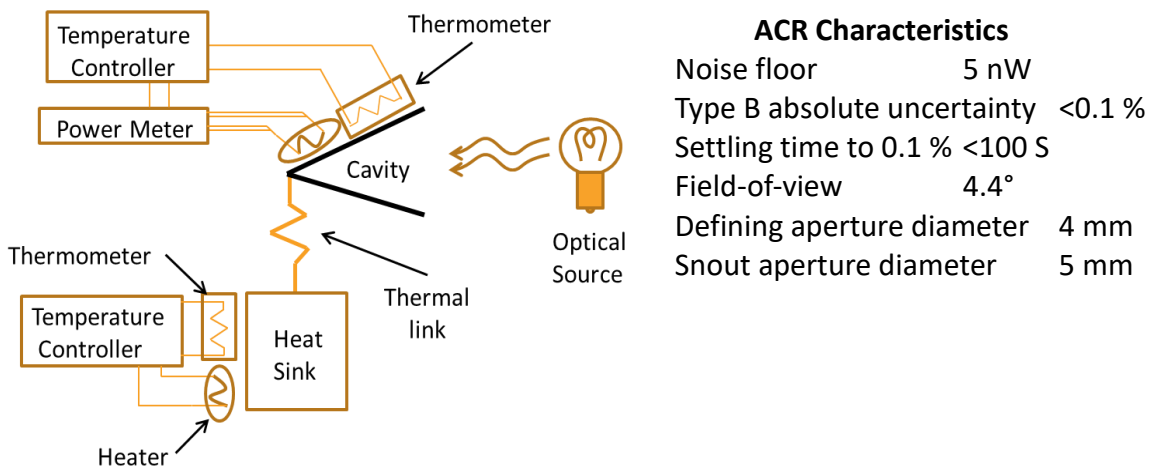
Figure 3-2 Left panel: Schematic illustrating ACR power measurement principle (electrical substitution). Right panel: Table of ACR design performance characteristics.

The cavity is a 30 degree cone painted black with a specular black paint that maximizes light trapping through multiple reflections, while minimizing light lost through diffuse reflection. Similarly designed cavities have achieved absorptance in excess of 0.9995. The small cavity size together with the use of negative temperature coefficient (NTC) thermistors and space qualified electronics support a noise floor of 5 nW when a 500 second measurement cycle is used. This corresponds to temperature control at a 10 µK resolution.

The NTC thermistors provide flexibility in choosing an operating temperature for the ACR cavity and ACR heat sink that is sufficiently above the maximum spacecraft operating temperature. Furthermore, these devices are expected to have less instrinsic 1/f noise than PTC sensors discussed for previous generation ACRs—albeit with less temperature sensitivity. Given the expected performance of the electronics, we have found that there is little advantage to the enhanced temperature sensitivity of the prior generation of PTC thermistors which had the added constraint of operating at a fixed temperature defined by the material's ferroelectric phase transition. The NTC thermistor resistances can be measured with a standard DC bridge circuit located on the ACR heat sink for maximum temperature stability. A 24 bit linear sigma delta A/D converter technology qualified for space provides wide temperature measurement range even with a ~1 uK electronic measurement resolution.

3.3.3 ACR Thermal Environment

Critical to the performance of the ACR is management of the changing thermal environment. 10ºC peak-to-peak temperature variation of the satellite housing can be expected in a low earth orbit experiencing eclipse. Any resulting variation in the thermal loading on the ACR cavity will appear as an unstable background that can easily mask the desired optical signal to be detected.

Our system is designed to limit background drift to about 10 nW equivalent detected optical power during each 500 second ACR measurement period. This is expected to meet our measurement uncertainty requirements since the greatest drifts in thermal background have a very large linear component that can be subtracted with a background measurement taken before and after the LED source illuminates the ACR (see Fig. 3-3).
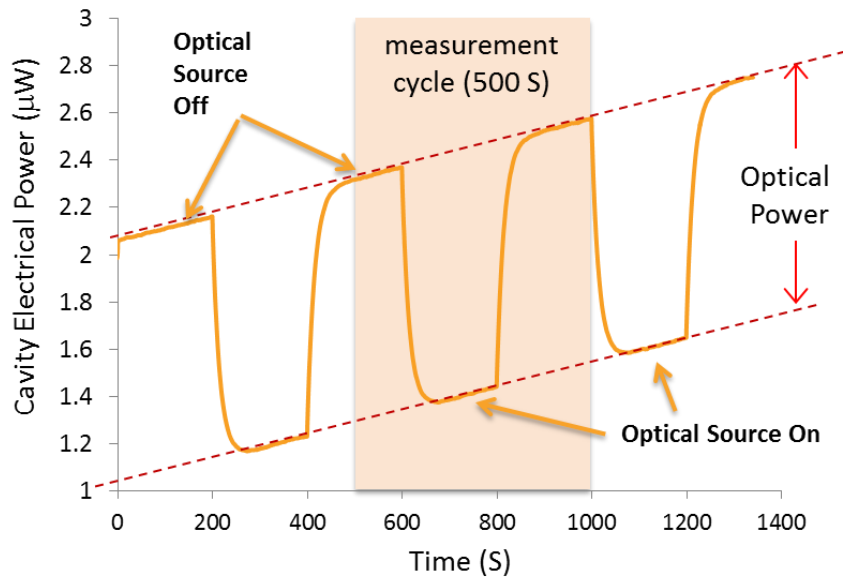
Figure 3-3: Simulated ACR measurement cycle illustrating a linear change of background starting and ending with a background measurement. Example shows 1 μW optical power.

Higher order non-linear fitting to the background variation is possible, as well. Data spanning 500 seconds is needed to complete background subtraction. Thus, a new LED wavelength emission can be re-calibrated every 600 seconds using this approach (6 calibrations per hour).

The ACR receiver has to be well isolated thermally so that its intrinsic noise performance can be realized. In order to minimize radiative coupling to the spacecraft, the receiver cavity is surrounded by a snout that is attached to the actively controlled heat sink (see Fig. 3-4). There are two snouts one inside the other that are both attached to the heat sink, but are otherwise isolated from each other. The outer snout acts as a guard that shunts radiative heat away from the inner snout, whose temperature more closely tracks the temperature of the controlled heat sink.
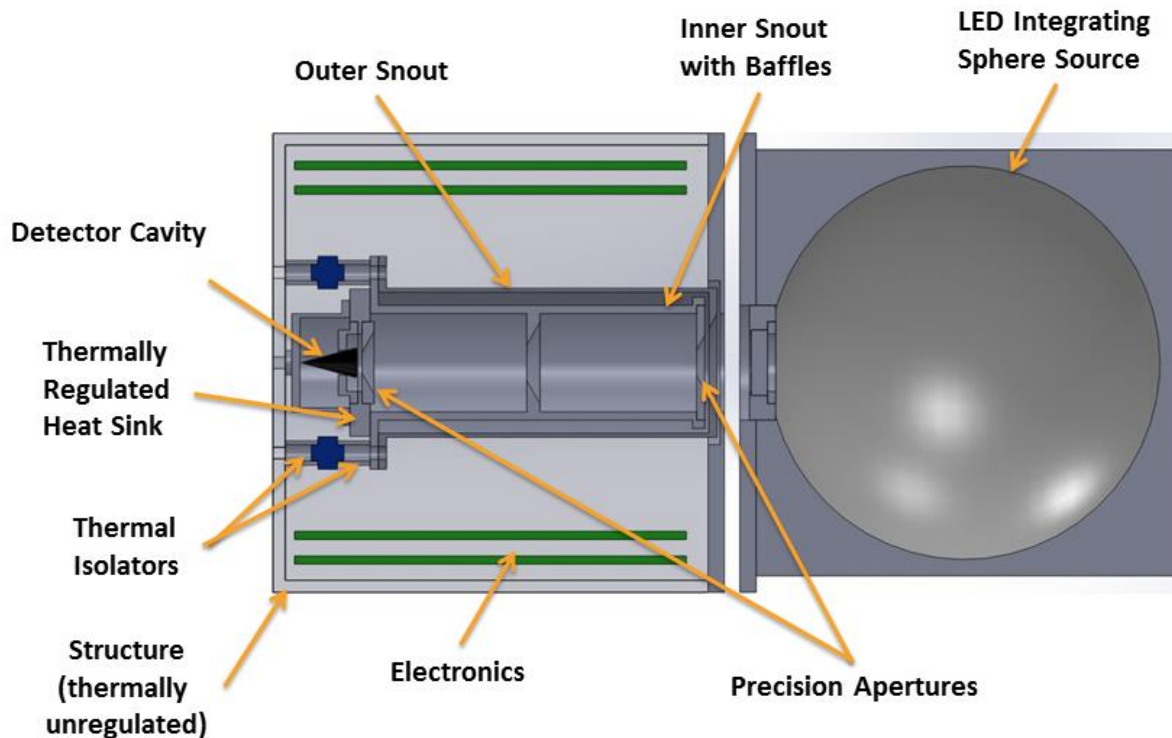
Figure 1-4: Cross-section drawing of the ACR with snout and monochromatic integrating sphere source. Temperature sensing electronics are located on the heat sink. Note that the other white light source and FTS remote sensor are not shown.

A 10 µK temperature stability of the heat sink over 10 minutes is desired. However, linear drifts in excess of this are tolerable as previously illustrated in Fig. 3-3. To minimize such drifts resulting from control errors and errors from varying loading from spacecraft temperature changes during a measurement cycle, a feed forward loop is included in the design. A thermometer placed near the heat sink standoffs, where the heat sink is most strongly coupled to the spacecraft is predictive of the thermal loading on the ACR because spacecraft temperatures are predictably driven by the orbit. Other temperature sensors around the housing are available for this purpose as well. An empirically derived feed forward heating signal is to be applied to secondary heaters located midway along the length of each thermal isolator to counter the effect of varying spacecraft temperature.

Since the ACR snout is tied to a well regulated heat sink on one end, a small temperature gradient can be induced along the length of the snout when a radiative load from spacecraft structure exists. The effect of a linear temperature gradient of the inner snout, expressed as the power radiated into the ACR cavity per unit temperature rise of the end cap, is about 20,000 nW/K. Thus, a 500 µK temperature gradient on inner snout causes 10 nW change in the ACR detected power).

However, we use a double snout as depicted in Figure 1-4. The outer snout protects the inner snout from developing any significant temperature gradient and thereby better stabilizes the background seen by the ACR cavity. A detailed analysis of this effect for the configuration illustrated in Figure 1-4 shows that the ACR cavity sensitivity to the surrounding spacecraft temperature is only 15 nW/K.

Another important sensitivity exists due to infrared radiation emitted from the integrating sphere that directly enters the ACR cavity. Our Phase 1 study has determined that the ACR cavity sensitivity to integrating sphere temperature is 130 nW/K.

These sensitivities to spacecraft thermal background are critical since they ultimately determine if the NIST-in-Space concept is feasible while using an un-cooled ACR and an un-cooled optical source. Furthermore, in order to keep ACR measurement error at least 3 times smaller than the desired 10 nW sensitivity needed by our system, then it is necessary that the integrating sphere temperature change remain linear to within 25 mK over 10 minutes.

This level of thermal stability is achievable using standard engineering design practice in an isolated and closed system having active thermal control as described above. Thus, we conclude that the NIST-in-Space concept of using an un-cooled ACR to measure 10 uW power levels to within 0.1% uncertainty is feasible.

3.3.4 Earth View Radiance Levels

The earth reflected solar radiance at 100% albedo represents our maximum detected signal for system design purposes. Table 3-1 summarizes the total power integrated over wavelength for several bands spanning the UV/VIS/NIR spectral range assuming 100% earth albedo radiance.

Note that the total integrated power is 51 µW which is a factor of 10,000 above our 5 nW ACR sensitivity threshold. Thus, calibration of the Earth viewing spectrometer to less than 0.1% uncertainty should be possible.

Wavelength Range	Sensor View 100% Earth Albedo (µW)
0 – 0.25 µm	0.6
0.25 – 0.3 µm	1.2
3.0 – 0.6 µm	17.7
0.6 – 1.2 µm	21.8
1.2 – 2.5 µm	8.2
2.5 – 5.0 µm	1.5
5.0 - 30 µm	0.3
Total	51

Table 3-1: Detected Optical Power at 100% Albedo by band for 2.5 cm aperture & 1 degree FOV

3.4 White Light Sources

Over the history of Earth observing sensors, several missions have used quartz tungsten halogen bulbs for calibration of the VIS/NIR spectrum (470 nm – 1900 nm). However, their broadband, smooth spectral output does not extend into the ultraviolet (250 – 470 nm). In addition, the spectral shape of the bulb emission is significantly mismatched to the solar spectrum as illustrated in Figure 3-5.
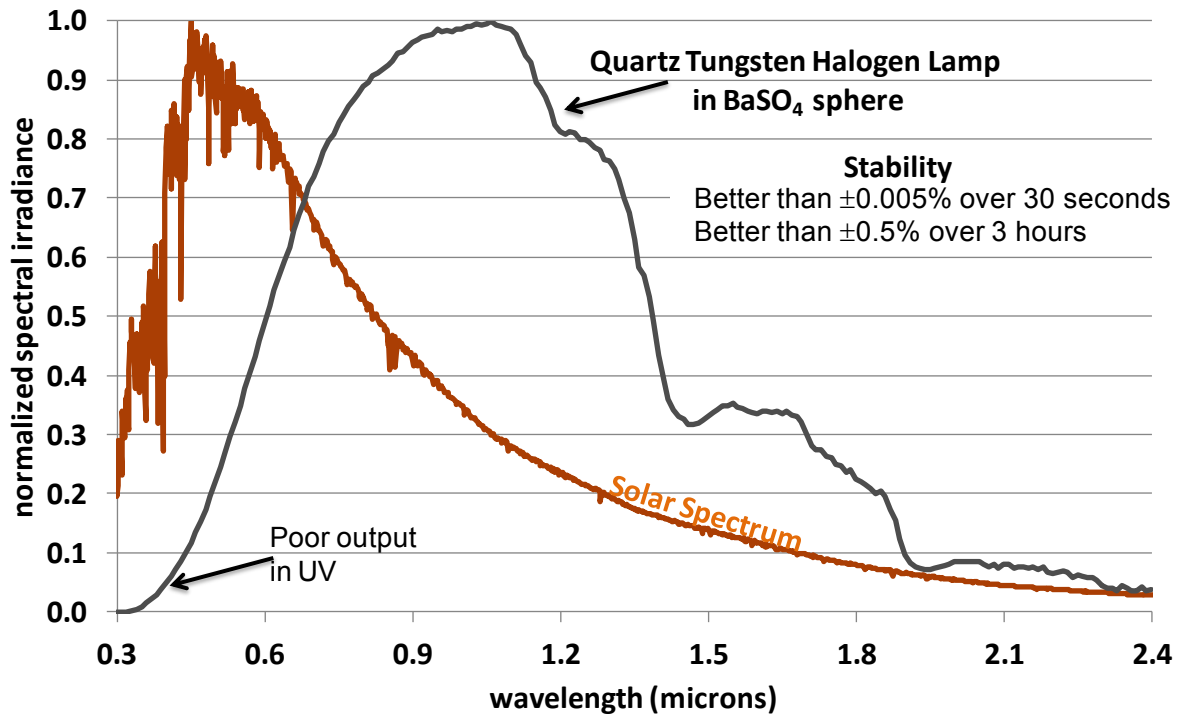
Figure 3-5: Quartz tungsten halogen bulb vs. solar spectrum

Deuterium lamps can be combined with quartz tungsten halogen lamps to produce an optical source with broader spectral coverage. Figure 3-6 shows a commercial version of this type of lamp fully integrated with a fiber optic output. Its spectrum is shown in figure 3-7. Note that this combination of light sources produces a minimum optical output were solar spectrum is at maximum. Thus, it too is mismatched for calibrating a system exposed to solar illumination that reflects at 100% earth albedo.

A new and much more promising technology for NIST-in-Space is the laser driven light source (LDLS) which is commercially available from Energetiq Technology Inc. (see Figure 3-8). This technology produces a very flat UV/VIS/NIR spectrum having high brightness [32]. The LDLS uses a 20 Watt, 1 μm wavelength CW diode laser module to directly heat a Xenon plasma to the 15,000 K temperature necessary for efficient deep ultraviolet production. In traditional approaches such as arc and deuterium lamps, the brightness, UV power, and lamp lifetime are limited by the use of electrodes to couple power to the plasma. The laser driven plasma is electrodeless and creates a small ~100 μm^3 plasma sphere with high brightness that allows efficient light collection over a broad spectral range from the deepest UV through visible and beyond. See the high quality flat spectrum in Figure 3-8 that is absent of features.

More importantly, LDLS enables extremely long lamp life compared to bulbs with electrodes. Lifetimes of 15,000 hours are typical at 30% reduced output. For NIST-in-Space, this source is operated intermittently thus making 10 year space missions with a plasma lamp possible.

Figure 3-6: Commercial deuterium with quartz tungsten halogen lamp & fiber optic
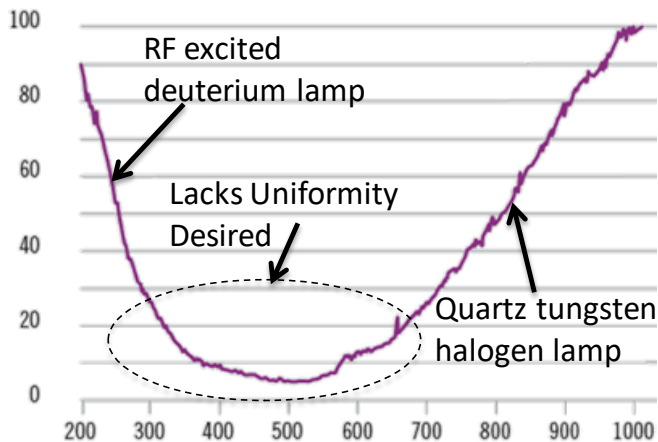
Figure 3-7: Deuterium & quartz tungsten halogen lamp spectrum
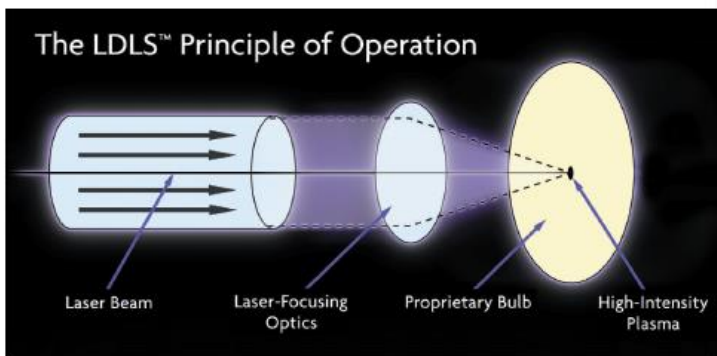
EQ-99FC Typical Performance:
with 230um diameter, 0.22NA, 1m long, solarization resistant fiber
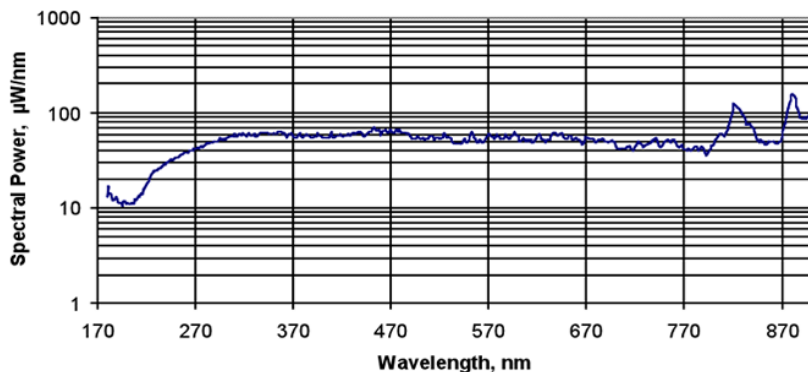
- **Flat spectrum (200 – 800 nm)**
- **Output range (200 – 2100 nm)**
- **Calibration accuracy +/-5% (95% confidence) 1000 hours**
- **Order of magnitude longer life over deuterium bulbs**

Figure 3-8: Laser driven plasma lamp produces flat spectrum over UV/VIS NIR bands

The commercial version of LDLS does not operate under vacuum and the position of the plasma within the lamp is also affected by orientation of the unit with respect to gravity. Operation of the commercial version in vacuum may also damage the optics since convective cooling of the unit would become ineffective under vacuum. However, these incompatibilities can be remedied with standard engineering design practice. The manufacturer of the LDLS equipment sees no fundamental obstacle in adapting this technology for space flight.

3.5 Monochromatic Sources

3.5.1 LEDs

Our "NIST in Space" concept relies on light emitting diodes as monochromatic light sources instead of tunable lasers. Technology currently exists to produce LEDs operating over the 260 nm – 3000 nm wavelength range. LEDs have also been qualified for operation in space.

The LEDs illuminate the interior of a highly reflective integrating sphere so that the multiple reflections internal to the sphere produce a spatially uniform radiance that can be viewed at the sphere's exit port. Using an integrating sphere is important for creating a radiance source having less than 0.1% non-uniformity. Consequently, when the ACR and FTS separately view the sphere's emission, then both will view the same radiance even if the aperture and Field of View (FOV) sizes are different for those respective instruments. In order to tie the sphere's radiance output to an international standard, the ACR view of the sphere radiance would be used.

There are many LED wavelengths available that span the 250 – 3000 nm spectrum. Figure 3-9 is a compilation from our Phase 1 study of the various LED wavelengths that can be used to produce monochromatic radiance sources for NIST-in-Space.   The integrating sphere in this example has a 7.62 cm diameter with highly reflective commercially standard $BaSO_4$ coating on its inner surface. The sphere exit port is 3 cm diameter.

The vertical axis of Figure 3-9 is the detected power for an FTS remote sensor which views either the earth or the LED integrating sphere source. The FTS has a 2.5 cm aperture and 1° FOV for this specific NIST-in-Space application, but other combinations of FOV size and aperture are possible.

The FTS spectral range is divided into 5 sub-octave detection bands so that a view of 100% earth albedo produces the 5 detected power levels (integrated over each band's wavelength range) shown for each of the respective bands. The FTS detected power for each of the LEDs is overlaid on this plot. Also superimposed on the plot is the 5 nW ACR detection performance threshold estimated from Section 3.3.2.

For the NIST-in-Space concept to be feasible, the red squares plotted in Figure 3-9 need to overlap with the blue triangles plotted. In other words, at each LED wavelength, the LED driven integrating sphere needs to produce the same optical radiance that 100% earth albedo produces when that radiance is integrated over each sub-octave band processed by the FTS. For most points plotted in Figure 3-9, the commercial off-the-shelf LEDs used in this preliminary analysis were underpowered by a factor of 100.

The LED optical power can be increased by combining multiple LEDs and using multiple injection points into the sphere. However, a factor of 100 is too large to be mitigated by this type of approach. Table 3-1 summarizes by wavelength the LED optical power used to produce the plots in figure 3-9. Table 3-1 also summarizes the total LED optical power needed to achieve 100% earth albedo radiance in each of the five FTS bands.
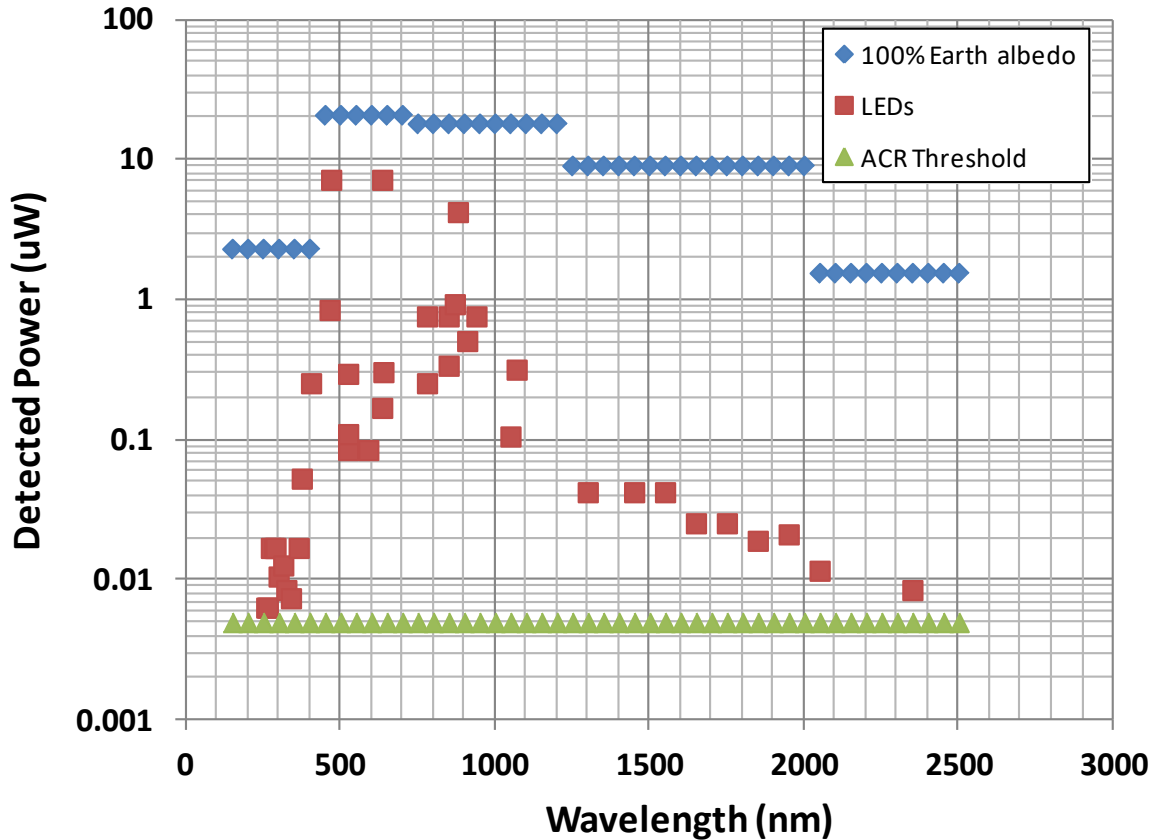
Figure 3-9: Total power detected by FTS instrument having 1° FOV and 2.5 cm aperture when viewing 100% earth albedo scene (blue) or when viewing LED driven integrating sphere (red). Note that commercially available LED chips used in this example are ~100x <u>underpowered</u>

Wave length	LED Optical Power		Wave length	LED Optical Power		Wave length	LED Optical Power		Wave length	LED Optical Power	
	Device	Need		Device	Need		Device	Need		Device	Need
nm	mW	mW	nm	mW	mW	nm	mW	mW	nm	mW	mW
260	0.3	109.3	405	6	493	780	6	428	1300	2	429
265	0.3	109.3	465	20	493	780	18	428	1450	2	429
275	0.8	109.3	470	170	493	850	8	428	1550	2	429
285	0.8	109.3	525	2	493	850	18	428	1650	1.2	429
290	0.8	109.3	525	2.6	493	870	22	428	1750	1.2	429
300	0.5	109.3	525	7	493	880	100	428	1850	0.9	429
315	0.6	109.3	590	2	493	910	12	428	1950	1	429
325	0.4	109.3	635	4	493	940	18	428			
340	0.35	109.3	635	170	493	1050	2.5	428	2050	1.1	147
365	0.8	109.3	639	7.2	493	1070	7.5	428	2350	0.8	147
375	2.5	109.3									

Table 3-1: LED device power used to generate Figure 3-9 versus LED optical power <u>needed</u> to yield 100% Earth albedo equivalent power for each of the five FTS spectral bands

In conclusion, the total LED device optical power needed to implement NIST-in-Space is as follows:

250 to 400 nm	100 mW optical power
400 to 2000 nm	500 mW optical power
2000 to 3000 nm	150 mW optical power

At these power levels, the selection of commercial off-the-shelf LED wavelengths will be more limited. However, these power levels are reasonably obtainable. Four identical wavelength LED devices each operating at one fourth the power could also be used. Use of four devices instead of one also enables four different injection locations into the sphere to improve radiance uniformity at the sphere exit port.

3.5.2 Monitor Detectors Solve LED Issues

LED output power degrades over time in the space radiation environment. The LED wavelength and optical power is also temperature sensitive. As such, LEDs cannot be relied upon to act as absolute wavelength or power standards. In addition, LED emission line widths are very broad in comparison to laser emission lines and the line width from an LED is often broader than the spectrometer channel that will be observing the line emission.

These limitations associated with LEDs are not a problem for the NIST-in-Space architecture because electrical feedback from monitor detectors within the integrating sphere is used to automatically level the LED emission to a fixed value. The monitor detector does not need to be accurate, only stable. Accurate knowledge of the emission line magnitude is provided by the ACR which views the radiance emitted by the LED/integrating sphere combination. Monitor detectors can then be used to replicate the LED power level at any time after the ACR calibration is complete. Figure 3-10 shows the spectral range covered by Si and InGaAs detectors. An InAs detector would monitor the 1.6 – 3.0 um range.
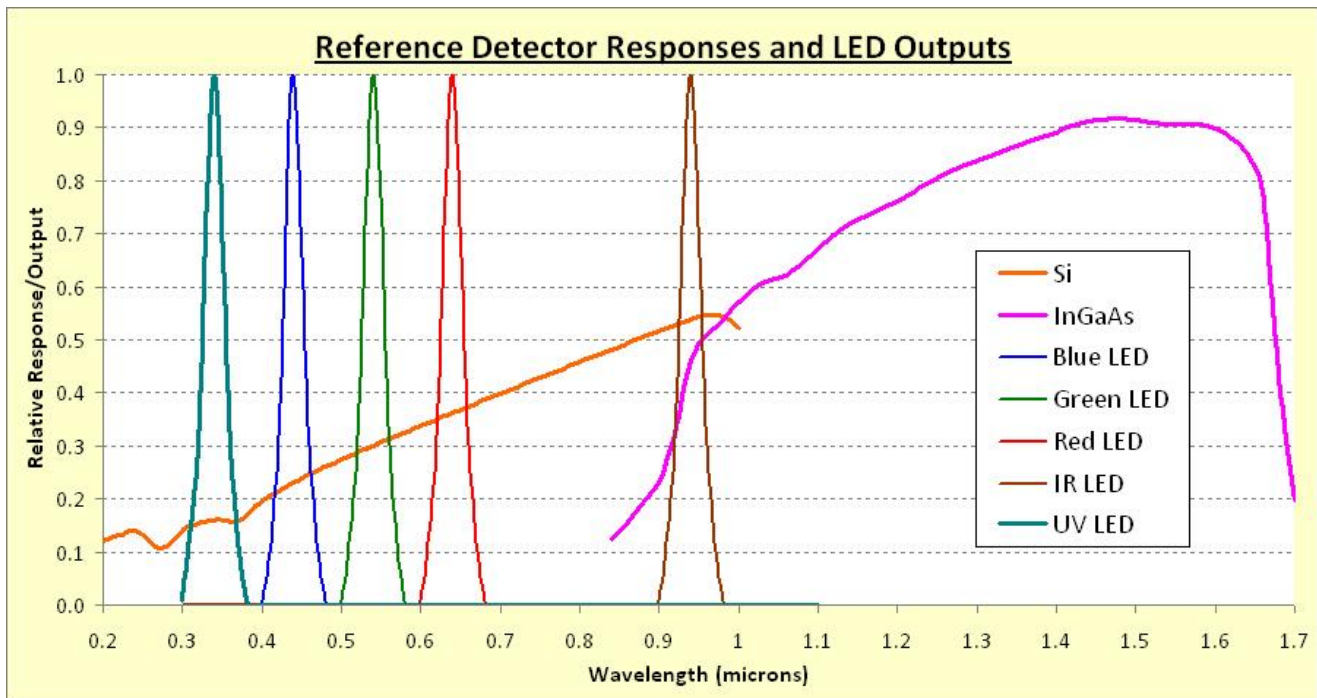
Figure 3-10: Five LED emission lines and response of Si and InGaAs monitor detectors

3.6 UV/VIS/NIR Fourier Transform Spectrometer

Table 3 2: Advantages of FTS Technology Over Grating or Prism based Spectrometers

1. Reproducible & precise wavenumber scale with inherent 1 ppm accuracy

2. One to three orders of magnitude finer spectral resolution/channelization

3. Spectral channels perfectly co registered to each image pixel

4. Multioctave wavenumber coverage possible within a single instrument

5. Avoids detector 1/f & popcorn noise common with DC coupled grating spectrometers

6. Greater than 10x better spectral response shape knowledge for each channel

7. Resultant spectrum is naturally Nyquist sampled (no information loss)

8. Identical spectral response for every channel in range (post processed in cm [1])

9. Nyquist sampled spectrum easily mapped to same exact wavenumber channel grid for multiple instruments in a mission

10. Mathematical synthesis of any arbitrary spectral response function from sinc(x) primatives

11. Flexibility to change spectral resolution and collection time by merely changing the sweep MPD (serving multiple missions with one instrument)

12. Spectral calibration is 50 to 100 times less sensitive to thermal variation

13. Optical component temperatures can be much higher for same sensitivity (very important for space applications in IR)

14. Detector temperatures can be much higher for same sensitivity (very important for space applications in IR)

15. Easier overall thermal cooling for hyperspectral imaging applications

16. Radiometric scale linearization of FTS to less than 0.02% uncertainty is possible by using a harmonic distortion processing method unique to FTS

3.6.1 Why an FTS?

Our NIST in space concept requires use of a Fourier Transform Spectrometer (FTS) remote sensor that operates over the wavelength range 250 – 3000 nm.

The FTS is preferred for the NIST-in-Space application over the more commonly used grating or prism spectrometer. In doing so, we bring 16 advantages of FTS technology to the UV/VIS/NIR bands which are summarized in Table 3-2.

Many of the advantages associated with FTS in Table 3-2 also imply that this technology should be preferred whenever the most accurate scientific measurements are sought. NIST-in-Space is all about making the most accurate and well calibrated spectrally resolved observations of the Earth.

However, the overriding reason an FTS must be used for NIST-in-Space is also the same reason why a grating spectrometer is incompatible with the NIST-in-Space concept. An FTS collects all optical energy from a band onto one detector. Sampling and signal processing methods then result in hundreds and even thousands of spectral channels from energy collected on one detector. This means that the FTS dynamic range is sized for much higher total photon flux onto the detector (Basically, all the photon energy in the band). This is fundamentally what makes the FTS compatible with an un-cooled ACR that has 5 nW noise threshold.

In contrast, a grating spectrometer has one detector for each spectral channel. Photon flux onto each detector of a grating spectrometer is typically more than two orders of magnitude lower than an equivalent FTS system. Thus, it is no longer possible to use LEDs with detected power 1000 times above the ACR noise threshold because this level of optical signal would saturate a grating spectrometer in every channel calibrated for a remote sensor designed to view the earth.

Since an FTS has a single detector for producing hundreds of spectral channels within a band, only 2 or 3 LED wavelengths are needed to trend the calibration for all those channels in a band. A grating spectrometer would need LED wavelengths for each grating spectrometer spectral channel…….or alternatively, a very spectrally flat, precision white light source for calibration.

Adjacent channels on FTS have very high correlation to each other from the standpoint of calibration since the same detector and electronics is used to process the photo current for all channels. This means LED wavelengths used for calibration do not need to be closely spaced when calibrating the FTS system.

3.6.2 Availability of UV/VIS/NIR Fourier Transform Spectrometers

Plane mirror Michelson FTS technology has been proven and widely used in infrared spectroscopy. However, adapting this technology for use at UV/VIS/NIR wavelengths has stagnated over the past 25 years. Previous attempts to make FTS practical for the UV/VIS bands have been hampered by the high electro-mechanical complexity of FTS, vibration sensitivity, inadequate metrology for metering the finely graduated OPD increments needed for operation at UV and by the 100 x tighter optical alignment tolerances needed as compared to FTS technology used for infrared operation.

Some organizations are working hard to bring the advantages of FTS technology to the ultraviolet and visible range. For example, NASA JPL completed a 2007 ROSES IIP to advance Imaging VIS FTS technology for panchromatic coverage using large 2D focal plane arrays, broadband optics and a porchswing mechanism supporting a large OPD[6, 7]. In 1998, prior work by NASA JPL resulted in the development of a UV/VIS FTS operating from 290nm - 675 nm installed in the JPL Table Mountain Facility[11]. This was an astronomy application in a very controlled vibration free environment.

In 2009, the Japanese Government successfully launched the Greenhouse gases Observing SATellite (GOSAT) [3, 4, 5] which carries the first FTS sensor in space that samples four narrow bands in the VIS to IR.

Currently, UV/VIS/NIR FTS instruments have few commercial suppliers [15, 16, 17, 28, 31] and all these products are designed for use in a stable lab environment. We found no suppliers for aerospace systems. Operation of UV/VIS/NIR FTS under modest vibration levels such as 1 milliG has not yet been accomplished with good results.

3.6.3 UV/VIS/NIR FTS for Aerospace Systems

3.6.3.1 FTS Architecture for NIST-in-Space

Our concept for a UV/VIS/NIR Fourier Transform Spectrometer is currently a TRL-2 (Technology Readiness Level) mature aerospace subsystem. We believe our FTS concept overcomes the prior obstacles identified in Section 3.6.2 that have stalled development of this technology for use in the UV/VIS/NIR spectral range. We also believe that our UV/VIS/NIR concept has promise to operate on aerospace platforms having modest vibration levels of 1 milliG.

The proposed FTS instrument is a plane mirror Michelson interferometer operating over the 200 nm to 3000 nm spectral range. The instrument has a 2.5 cm input aperture and 1° FOV that produces a 10.5 km ground footprint if operated from a 600 km earth orbit. A commercially available, state-of-the-art piezo actuator translates the Michelson mirror by ±900 μm, thus producing a 0.7 cm^{-1} spectral resolution (equivalent to 0.024 nm resolution at a 400 nm wavelength). This spectral resolution is an order of magnitude finer than typical grating spectrometers operating in the UV.

Unlike interferometers using porch swing, wishbone or flex pivot mechanical mechanisms, our interferometer dynamically aligned piezo actuator is very stiff and resonant free below 1 kHz. Thus, external vibrations don't convert into relative motion within the interferometer. The piezo actuator combines with small interferometer size and unibody construction to make the entire assembly very insensitive to vibration. We believe it can be designed resonant-free up to 700 Hz.

Figure 3-11 illustrates the FTS concept. The main optical system combines the FTS with a telescope to focus the light onto a small diameter field stop. A band pass filter (not shown), located after the field stop sets the spectral range. Energy then passes through a field lens. The detector is positioned at the resulting exit pupil. The field stop and field lens may be replaced in the future with an N x N detector array for hyperspectral imaging applications. Four different detector materials are used to cover the full UV/VIS/NIR range with good sensitivity: Band 1 (200 - 400 nm), Band 2 (400 - 1100 nm), Band 3 (800-1700 nm) and Band 4 (1700-3000 nm).

Interferometer beamsplitter and compensator plates are made from one substrate material that enabling full 200 nm - 3000 nm spectral coverage. One path of the interferometer uses a moving plane mirror combined with a dynamic tip/tilt piezo to create an optical path difference while still maintaining precise optical alignment. The other optical path uses a fixed mirror to establish the FTS line-of-sight. Laser metrology is used to measure alignment and control the piezo actuators.
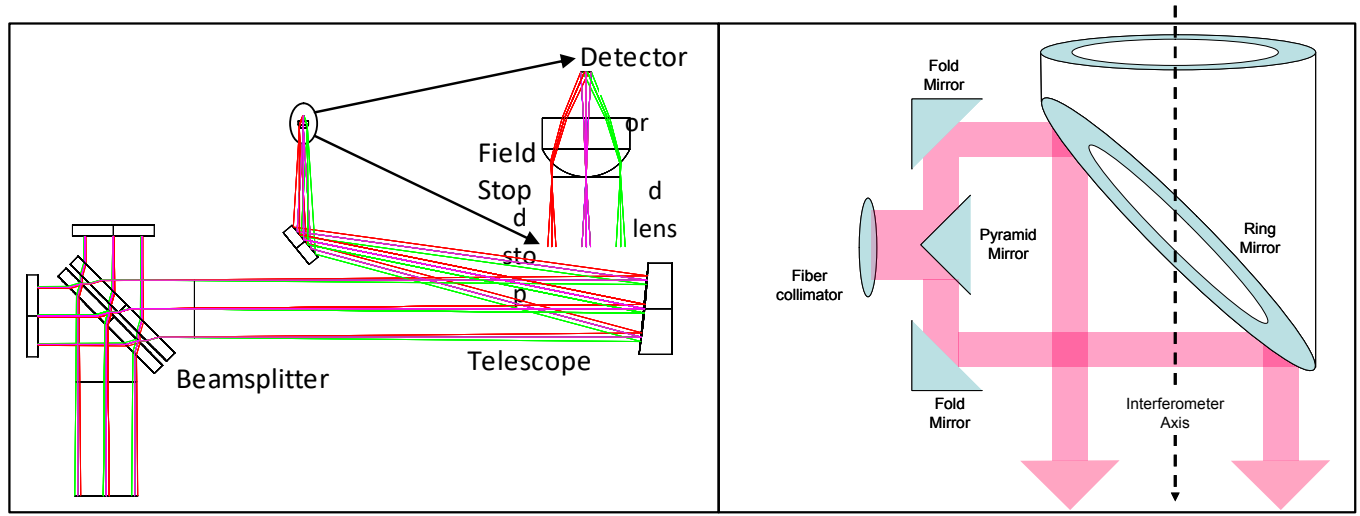
Figure 3-11: UV/VIS/NIR Optical configuration and laser metrology (only one band shown)

One enabling technology is the laser metrology system illustrated in Figure 3-11. A standard 1550 nm telecom laser diode is fed via single-mode fiber to a fiber collimator producing a ~4 mm diameter beam. The beam is incident on a 4 sided pyramidal mirror that divides the beam into four separate paths perpendicular to the incident beam and separated by 90 degrees. Each of those four beams strikes a 90 degree fold mirror mounted on a ring. The four paths are now parallel to each other and injected concentric to the interferometer axis. The four beams exit the interferometer modulated by tilt/tip misalignment and OPD changes. We expect this geometry to allow tip/tilt dynamic alignment to be controlled to the 0.025 μrad stability needed during the UV interferogram collection process.

3.6.3.2 Enabling Technologies for UV/VIS/NIR FTS

Five enabling technologies were identified during this Phase 1 which we believe make a generic breakthrough in UV/VIS/NIR spectrometer operation feasible for aerospace missions. These would include:

1. Recent advancements in piezo electric transducer technology currently available commercially that enable the larger interferometer mirror displacements needed for 0.7 cm^{-1} resolution in UV/VIS/NIR (i.e. 0.024 nm resolution @ 400 nm)

2. Combining very stiff piezo transducers with unibody interferometer construction to yield 1 milliG vibration immunity of the FTS when operated at UV wavelengths

3. Novel laser metrology geometry and processing that can maintain the 100 x more stringent optical alignment needed for a plane mirror Michelson interferometer operating at UV wavelengths

4. Combining a piezo actuator adaptive repetitive control algorithm with a vibration robust structure in order to produce an extremely smooth linear translation of the Michelson mirror. An accurate, uniform, 36 nm OPD metrology sampling increment of interferograms then becomes possible by interpolating laser metrology fringe count twenty fold.

5. Digital processing & interpolation methods that permit FTS detectors to be sampled at a fast fixed clock rate followed by conversion to the desired fixed increment OPD sampling of interferograms

In combination, we believe these five technologies can overcome all remaining obstacles that have stagnated UV/VIS FTS advancement over the past 25 years as discussed in Section 3.6.2. To our knowledge, a UV/VIS/NIR FTS instrument that combines all five of the enabling technologies listed above has never been built.   Therefore, we estimate the technology readiness to be at TRL2.

3.6.3.3 Future UV/VIS/NIR FTS Development

As described above, the enabling technologies that make UV/VIS/NIR FTS operation feasible for use in aerospace systems outside the laboratory represent incremental but extremely important advances since such a system has never been built and since the benefits (Table 3-2) of UV/VIS/NIR FTS technology can impact a broad range of science applications in addition to NIST-in-Space. Hence, further development through prototype demonstration is recommended following this NIAC Phase 1 study.

4. Low Earth Orbit Remote Sensor Concept

4.1 System Configuration

Figure 4-1 illustrates how the NIST-in-Space concept would be implemented as a cross-track earth scanning remote sensor. This notional system would fit within a 10 cm x 20 cm by 30 cm volume corresponding to the size of a 6U Cubesat. A separate electronics module (not shown) is also needed for power conditioning, communication, telemetry, servo control, interferogram data processing and for generation of laser power to excite the white light plasma source.

The LED driven integrating sphere is excited by any of 15 LED wavelengths within the range 250 to 3000 nm. This sphere can also mechanically rotate 90° so that its exit port is aligned either to the ACR or to the scanning FTS.

The Fourier transform spectrometer step scans the earth in a Cross-track direction to produce 30 separate spectrometer measurements across the earth surface. Rotation of the entire Fourier Transform Spectrometer is desirable in order to preserve polarization characteristics of the remote sensor for all 30 cross-track measurements. The size of the IFOV is 14 km at nadir from an 833 km JPSS sun synchronous earth orbit which produces a cross-track swath of 2200 km. A 10 km footprint is produced at a 600 km orbit and a 6.6 km footprint from a mount on the International Space Station.
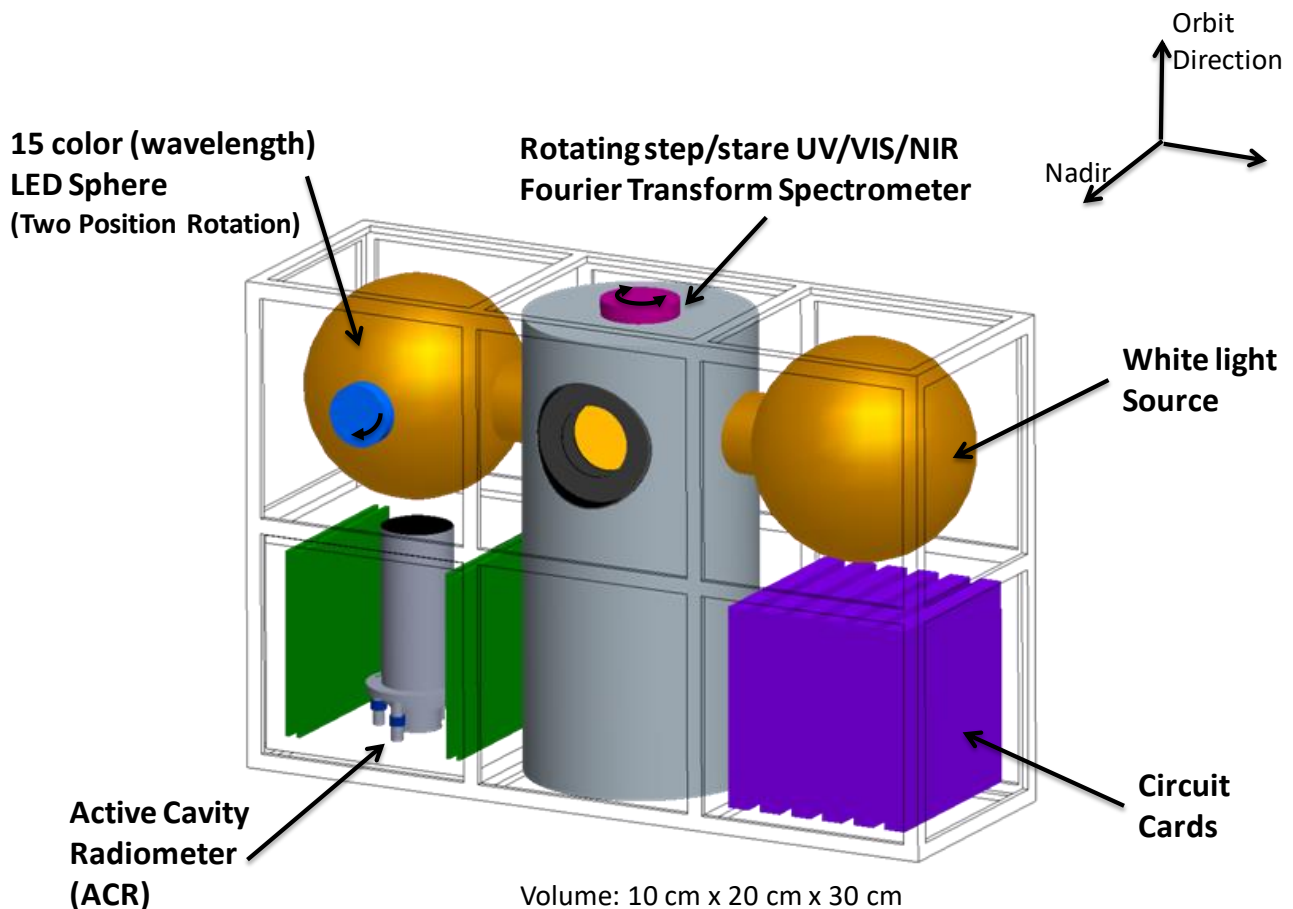

Figure 4-1: NIST-in-Space implemented as a Cross-track Earth scanner

4.2 Calibration Timeline for SI Traceability

Figure 4-2 shows the position of the LED driven integrating sphere when it is being calibrated by the ACR. The ACR must view the integrating sphere for 10 minutes in order to calibrate the radiance associated with one LED wavelength. The 10 minute measurement sequence is composed of three steps. All LEDs are powered OFF for 200 seconds, followed by one LED powered ON for 200 seconds, followed by all LEDs powered OFF again for 200 seconds. This allows the UV/VIS/NIR radiance produced by the LED to be calibrated while also subtracting the variable IR background produced from an un-cooled sphere and un-cooled ACR (see Section 3.2.2). A monitor detector within the sphere that is insensitive to the changing thermal background records the calibrated optical signal level so it can be reproduced at any time afterwards without viewing the ACR.

Fourier Transform Spectrometer (FTS)

10 minutes to calibrate each LED radiance

Process repeats for 15 LED wavelengths (265 nm – 3000 nm)

Monitor detectors within sphere remember each wavelength calibration for quick recall during normal FTS scanning
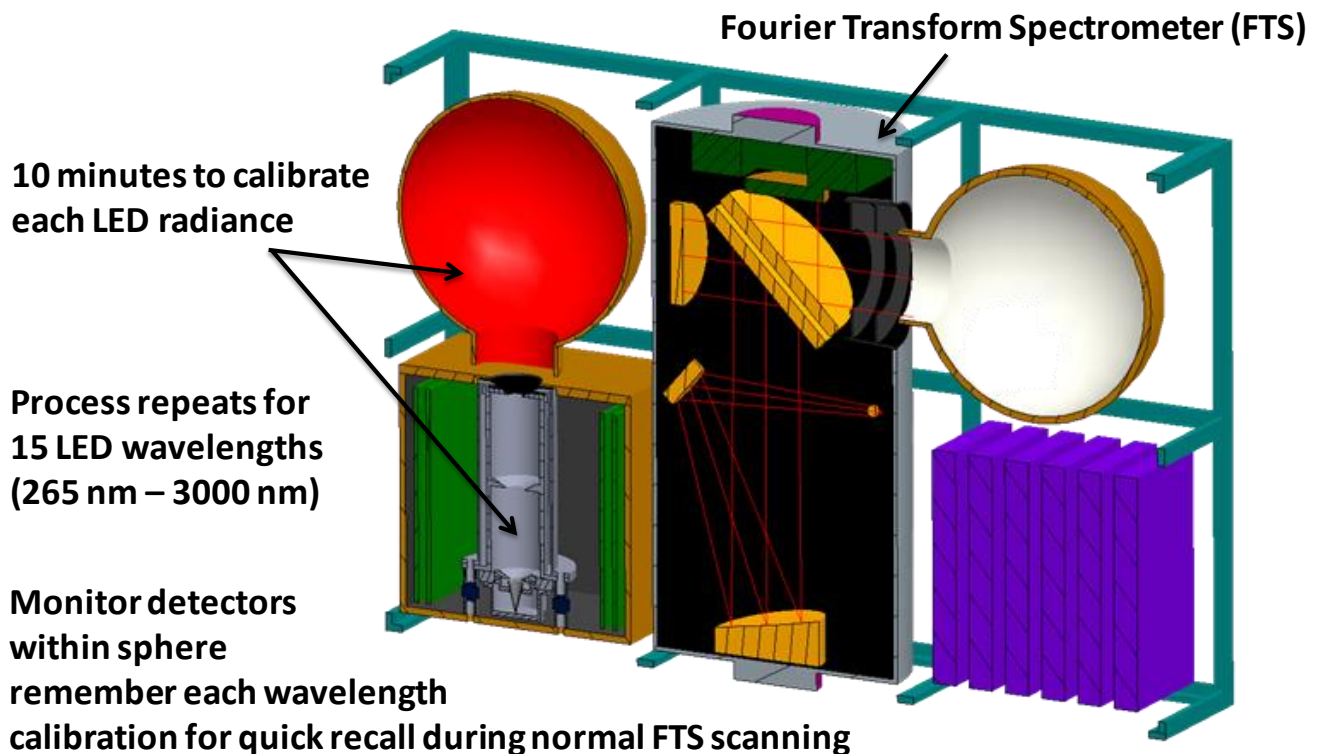
Figure 4-2: FTS scans earth and white light source while LED Sphere undergoes NIST traceable calibration by ACR

Fifteen LED wavelengths are available to provide calibration points throughout the 250 – 3000 nm spectrum. Each wavelength requires 600 seconds to recalibrate its associated radiance level.

After an LED calibration by the ACR, the sphere is mechanically rotated 90º so that the cross-track scanning FTS can now view this sphere's radiance once every cross-track sweep over the next 200 seconds. All 15 LED radiance levels are recalled one at a time and cycled through during this 200 second view opportunity. Thus, each successive cross-track sweep of the FTS will view a different LED wavelength radiance that is traceable to SI during this 200 second view. All of this occurs while the FTS is still performing normal earth scans.

This process repeats for the duration of the space mission so that the FTS calibration is updated with SI traceability at 15 specific wavelengths across the 250 – 3000 nm range every 800 seconds (13.3 minutes). In addition, by using this process each LED wavelength gets recalibrated by the ACR once every 200 minutes in order to preserve the SI traceability indefinitely. Monitor detectors within the sphere assure that the ACR calibration of each LED is preserved and accurately reproduced over the 200 minute interval spanning ACR re-calibrations.

4.3 Calibration Timeline for White Light & Black Target Source

Figure 4-2 shows a white light source (integrating sphere) always providing a view to the FTS. Similarly, a black target view (not shown in figure 4-2) is also always available to the FTS. These two targets provide recalibration of the FTS for all wavenumber channels over the 250 to 3000 nm spectral range.

The white light source is chosen to provide a smooth continuous spectrum as previously described in Section 3.4. It should be noted that the use of an integrating sphere to produce a white light reference is notional. If the laser driven plasma source (Figure 3-8) is used as a white light reference, then the integrating sphere would be replaced by a collimator with its point of focus on the bulb plasma. The output of this collimator produces full aperture illumination of the FTS.

Calibration accuracy of the white light source is not important. This is because the spectral response of the FTS to the white light source will be resolved against the 15 SI traceable LED wavelength radiances provided by the LED driven integrating sphere. In essence, the white light source allows the system to accurately interpolate the calibration to all spectrometer channels with 15 anchor points to SI traceability. The white light source is not required to be perfectly uniform over the FTS aperture.

Since we desire operation over 10 year mission durations and since all white light sources have a limited operating life, then it becomes necessary to keep the white light source duty cycle sufficiently low in order to preserve the bulb's operating life. The laser driven plasma source has the best lifetime compared to any other alternative available and it also has the best spectral characteristics for UV/VIS/NIR calibration (Section 3-4). This plasma source is currently estimated to have a three sigma lifetime of 15,000 hours and could therefore be operated at a 17% duty cycle for reliable operation in space over 10 years.

We expect the radiance produced from this source to degrade slowly by about 30% over its lifetime. This is acceptable since all changes in radiance level from this source are calibrated out of our system by intercomparison with the 15 LED SI traceable radiances.

Our current plan is to operate this white light source for 15 minutes once every 101 minute orbit period. Most of the 15 minute ON time is used to warm up and stabilize the laser driven plasma prior to making a full spectrum calibration near the end of the 15 minutes. In addition, it should be noted that the 15 LED SI traceable calibrations will repeat more frequently (once every 13.3 minutes). Thus, the responsivity of the FTS only needs to remain stable over this shorter time interval.

The black target reference used for calibration is viewed during every FTS cross-track sweep. This eliminates all calibration errors due to offset drift of the FTS electronics and detector. Furthermore, the FTS instrument only processes an AC signal interferogram making the FTS naturally immune to electronic/detector offset drift.........another advantage of using FTS instead of a grating spectrometer as the NIST-in-Space remote sensor.

Our past experience at Exelis in designing, building and testing space flight infrared FTS instruments demonstrates that FTS remote sensors can be designed with excellent response stability over 13.3 minute

intervals. We believe this engineered capability can be extended to UV/VIS/NIR FTS remote sensors to make NIST-in-Space possible.

4.4 FTS Operating Timeline

Our proposed FTS remote sensor has the performance characteristics summarized in Figure 4-3. The entire FTS instrument is housed in a rotating tube that permits the line-of-sight to be step scanned across the earth as well as the various calibration targets used for NIST-in-Space. An interferogram is collected once every 200 ms for the FTS described in Figure 4-3. This breaks down into 190 msec for interferogram collection and 10 msec for stepping. Each Cross-track scan of the earth including calibration views is completed in eight seconds.

Further development of the FTS optical design is needed to accommodate multiple bands/detectors, stray light control, dual polarization detection and accommodation of electromechanical actuators to do the earth scanning. No effort in our NIAC Phase 1 study was placed into developing these conventional engineering aspects of the FTS remote sensor. Instead, we devoted effort to identifying the five major risks associated with making UV/VIS/NIR FTS feasible for aerospace systems as described in Section 3.6.

Interferometer

- > Plane mirror Michelson with dynamic alignment
- > Beam splitter   200 nm – 3000 nm
- > FOV size   1°
- > Resolution   0.7 cm^{-1}
- > Mechanism   z, tip, tilt piezo
- > Sweep rate   0.1 cm/sec

Metrology

- > Laser diode   1550 nm
- > Sampling   38.75 nm
- > Interpolation 20x

Detectors

- > GaP   200 – 555 nm
- > Si   400 – 1100 nm
- > InGaAs 780 – 1700 nm
- > InAs   1500 – 3000 nm

z, tip, tilt piezo driven mirror

fixed mirror

Beam splitter

Detector

telescope

Preliminary FTS notional Concept
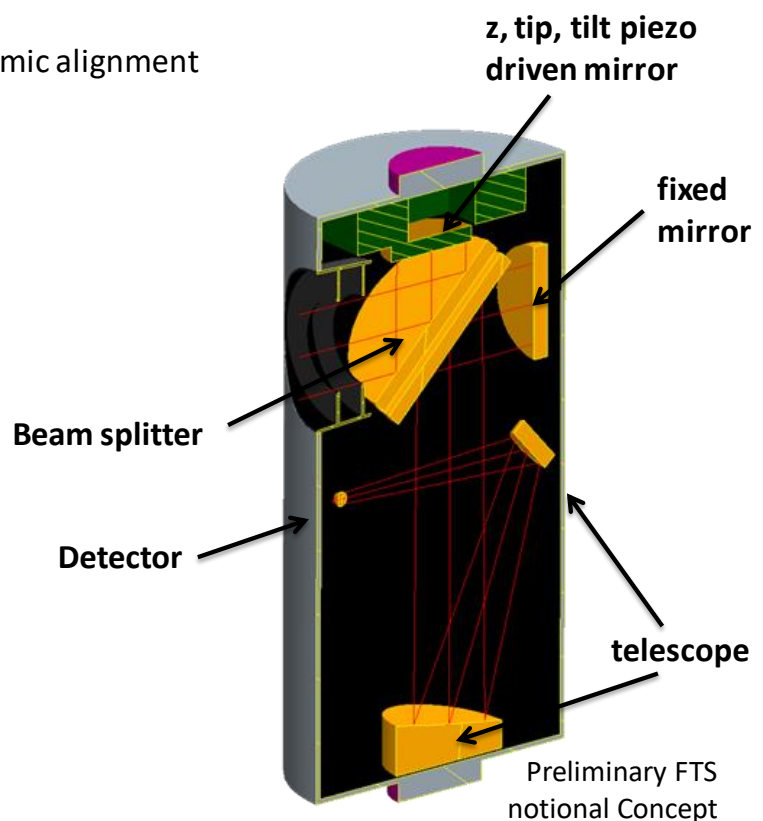
Figure 4-3: UV/VIS/NIR Fourier Transform Spectrometer Concept

5. Cubesat Simulation

An on-orbit demonstration that combines our ACR with the LED driven integrating sphere is a very attractive experiment for a future low-cost Cubesat project. Figure 5-1 illustrates the idea.

A 3U Cubesat (10 cm x 10 cm x 30 cm) can accommodate our ACR and LED integrating sphere while also allowing the rest of the Cubesat volume to be dedicated for spacecraft overhead functions. The objective of this demonstration is to show that the ACR can achieve the 5 nW measurement accuracy needed to make NIST-in-Space possible.

3U CubeSat Configuration
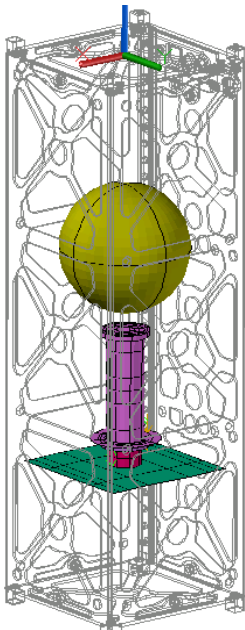
Passive magnetic orientation of CubeSat during an orbit
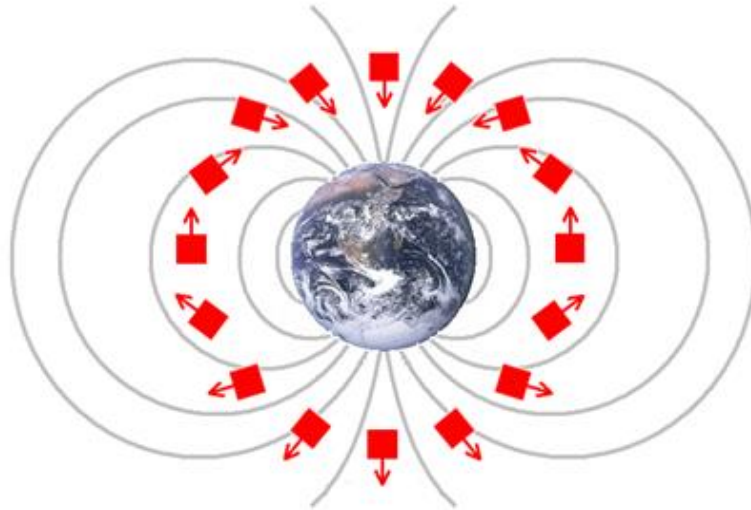
Two different sun-synchronous orbits simulated
- 800 km eclipse
- 800 km non-eclipse

Figure 5-1 Left panel: ACR and LED Sphere inside a 3U Cubesat. Right Panel: Cubesat tumbles twice per orbit due to orientation to earth's magnetic field

A small satellite such as a Cubesat is an excellent way to show this capability because the temperature variation of a low earth orbit satellite having low mass is a more difficult case as compared to a larger satellite that can better control the thermal environment.

Figure 5-2 plots the satellite temperature variation simulated during this NIAC Phase 1 study at various locations within the Cubesat in order to evaluate if a future Cubesat demonstration would be worth pursuing. We find that the expected temperature change of the satellite envelope is 25ºC peak-to-peak and that the temperature change at the ACR mount is 10ºC peak-to-peak with one cycle per orbit. This would be a challenging and suitable thermal environment to demonstrate ACR operation.
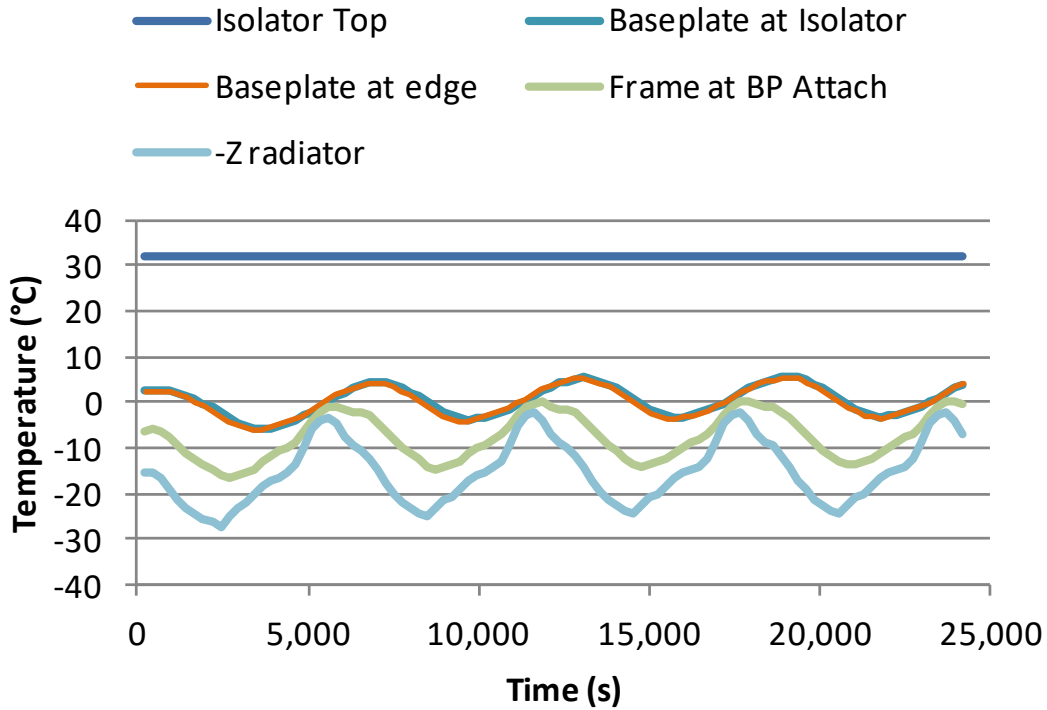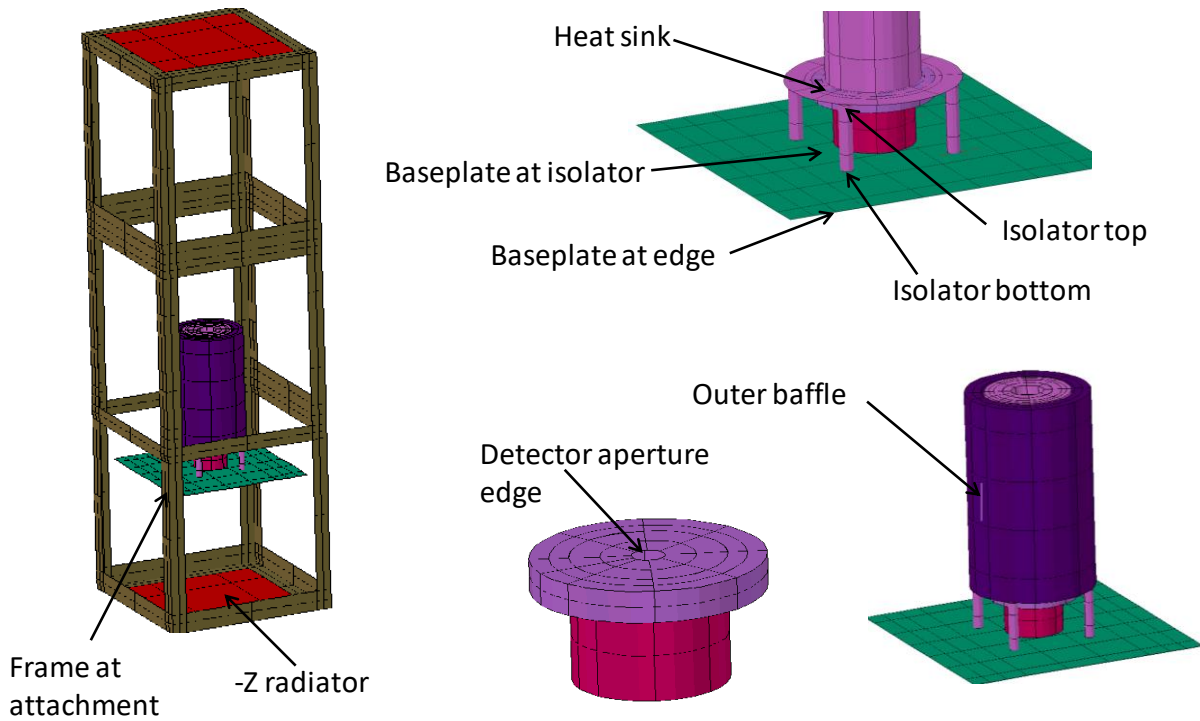
Figure 5-2: Thermal simulation of 3U Cubesat ACR & LED integrating sphere operating in an 800 km eclipse orbit

The Cubesat experiment would use a select number of LED wavelengths to illuminate the integrating sphere. The normal ACR measurement cycle previously illustrated in Figure 3-3 would be used. When an LED is ON, the output radiance of the sphere is stabilized to a fixed value by monitor detectors within the sphere. The monitor detectors assure that the radiance is stable over the entire orbit even when temperatures are changing.

The absolute knowledge of what radiance level exists in then provided by the ACR measurement. The ACR should produce the same reading over the entire orbit so that the differences in these readings are always less than 5 nW. If this can be accomplished with a Cubesat demonstration, then the ACR readout accuracy is demonstrated in a worst case thermal environment.

Furthermore, the technology readiness level is raised to TRL8.

6. NIAC Phase 1 Study Accomplishments

We successfully accomplished what we set out to do in our research plan previously described in Section 1.3

- Showed 0.1% ACR calibration can be achieve without cryogenic cooling

- Showed calibration can be achieved at 100% earth albedo radiance level

- Components are available for sources: LEDs, fiber optics, integrating spheres and lamps

- Thermal background stability & background cancellation methods make the broadband ACR effective as a UV/VIS/NIR radiance meter while using an <u>un-cooled</u> visible source

- We combined the above properties into a well defined UV/VIS/NIR hyperspectral system concept backed by analysis & achievable subsystem requirements

A more detailed technical summary of our findings from this NIAC Phase 1 study was previously summarized in Section 1.4. We believe we have advanced the NIST-in-Space concept from TRL2 to TRL3 and this research is ready to progress to the next phase.

Subsequent Phase 2 NIAC research would focus on prototype builds, experimental verification and further UV/VIS/NIR FTS remote sensor feasibility analysis/definition.

7. Statement of Patentability & Public Release

There are no patentable items claimed by Exelis Inc. and L-1 Standards and Technology in the performance of this grant. The contents of this report are intended for release to the public domain and free of any proprietary content. This document does not contain ITAR restricted technical data.

8.   References

1) Hengstberger F., *Absolute Radiometry*, San Diego,Academic Press, 1989.

2) Parr A. C., A National Measurement System forRadiometry, Photometry, and Pyrometry Based Upon Absolute Detectors, *NIST Tech. Note 1421*, 1996.

3) Initial Onboard Performance of TANSO-FTS on GOSAT, 2009 Optical Society of America, Kuze, Suto, Nakajima, Hamazaki

4) Prelaunch performance test results of TANSO-FTS and CAI on GOSAT, Proceedings of SPIE Vol. 7082 708214-1, Yashida, Kawashima, Ishida, Hamada, Tanii, Katsuyama, Suto, Kuze, Nakajima, ZHamazaki

5) Noise Modeling for the TANSO-FTS sensor aboard GOSAT, 2007 Optical Society of America, Tomosada, Kuze, Tsubaki, Yokota

6) An Imaging Fourier Transform Spectrometer for the Geostationary Coastal and Air Pollution Events (GEO-CAPE) Mission, NASA JPL presentation, 23 September 2009, Eldering, Key, Sander

7) Panchromatic Fourier Transform Spectrometer for the GEO-CAPE Mission, NASA Earth Science Technology Forum presentation 2010 made by NASA JPL, Sander, Beer, Blavier, Bowman, Eldering, Key, Rider, Toon

8) P.Connes and G. Michel, Applied Optics 14 (1975) 2067

9) A.Y. Irfan, A. P. Thorne, R. A. Bohlander and H.A. Gebbie, J. Phys. E: Sci. Instrum. 12 (1979) 472

10) Laser Controlled Sampling in a Fourier Spectrometer for the Visible and Ultraviolet using a Phase Lock Loop, Optics Communications Vol. 45, number 6 (1983)

11) High Resolution Fourier Transform Ultraviolet-visible spectrometer for the measurement of atmospheric trace species: application to OH; Optical Society of America, Applied Optics/ Vol. 40, No. 12 (2001)

12) 12. Beam Folding Ultraviolet-visible Fourier Transform Spectrometry and Underwater Cytometry for in situ Measurement of Marine Phytoplankton; Xuzhu Wang, Doctor of Philosophy Thesis, Hong Kong Baptist University (2007)

13) Near UV-near IR Fourier Transform Spectrometer using the beam folding position tracking method based on retroreflectors; Xuzhu Wang, Robert Chan, Amelia Cheng; American Institute of Physics, Revie of Scientific Instruments 79, 123108 (2008)

14) Tests of a practical visible-NIR imaging Fourier transform spectrometer for biological and chemical fluorescence emission measurements; Jianping Li, Robert Chan, Xuzhu Wang; Optical Society of America, (2009) Vol. 17, No. 23/OPTICS EXPRESS 21083

15) Visible Imaging Fourier Transform Spectrometer: Design and Calibration; Wishnow, Wurtz, Blais-Ouellette, Cook, Carr, Lewis, Grandmont, Stubbs; Proc. of SPIE, Vol. 4841

16) Stratospheric Trace Gas Measurements in the Near UV and Visible Spectral range with the Sun as a Light Source Using a Fourier Transform Spectrometer; Notholt & Pfeilsticker, Society for Applied Spectroscopy, Applied Spectroscopy Vol. 50, No. 5 (1996)

17) Imaging Fourier Transform Spectrometer for Visible Band Astronomy; Wishnow, Wurtz, Cook, Carr, OSA/FTS 2005

18) Efficient Algorithm to Correct for Tilt Disturbances on FTS Data
OSA – FTS & Optical Remote Sensing of the Atmosphere Topical Meeting, 2003

19) Celestial body irradiance determination from an underfilled satellite radiometer: application to albedo and thermal emission measurements of the Moon using CERES: Grant Mathews, (2008), OSA, Applied Optics, Vol.47, No. 27

20) Absolute Irradiance of the Moon for On-orbit Calibration; Stone & Kieffer, http://www.moon-cal.org/references/pdf/Seattle2002.pdf

21) Spectral Irradiance and Radiance Responsivity Calibrations using Uniform Sources (SIRCUS) http://www.nist.gov/physlab/div844/grp06/sircus_facility.cfm

22) MODIS On-orbit Calibration and Characterization; Xiong, Chiang, Guenther, Barnes

23) MODIS Reflective Solar Bands Calibration Algorithm and On-orbit Performance; Xiong, Chiang, Guenther, Barnes; Proc. of SPIE (2003) http://mcst.gsfc.nasa.gov/uploads/files/SPIE_CHINA_RSB.pdf

24) Spectralon diffusers used as in-flight optical calibration hardware; Chommeloux, Baudin, Gourmelon, Bezy, Van Eijk-Olij, Schaarsberg, Werij, Zoutman; SPIE conference on long term degradation of optical systems, SPIE Vol. 3427   0277

25) Meris Diffuser Calibration at TNO TPD; Courrèges-Lacoste, Schaarsberg, Van Eijk-Olij http://envisat.esa.int/workshops/validation_12_02/proceedings/meris/03_bazalgette.pdf

26) Multi-angle Imaging SpectroRadiometer (MISR) On-Board Calibrator (OBC) In-flight Performance Studies; Nadine L. Chrien, Carol J. Bruegge, and Robert R. Ando; IEEE TRANSACTIONS ON GEOSCIENCE AND REMOTE SENSING, VOL. 40, NO. 7, 2002

27) On-orbit Performance of the Earth Observing System Moderate Resolution Imaging Spectroradiometer; 1st year of data, B. Guenther[a] , X. Xiong[b], V. V. Salomonson[a], W. L. Barnes[a] and James Young; Remote Sensing of Environment, Volume 83, Issues 1-2, November 2002, Pages 16-30

28) FTS6000 http://saf.chem.ox.ac.uk/Instruments/FTIR/FTSoptprin.html

29) Solar Radiation and Climate Experiment (SORCE) , http://lasp.colorado.edu/sorce/index.htm

30) A new, lower value of total solar irradiance: Evidence and climate significance, G. Kopp and J. Lean, GEOPHYSICAL RESEARCH LETTERS, VOL. 38, L01706, doi:10.1029/2010GL045777, 2011

31) http://www.bruker.com/en/products/molecular-vibrational-spectroscopy/ftir/ifs125-series/overview.html

32) http://www.energetiq.com/html/eq99FC.html#

33) Active cavity absolute radiometer based on high Tc superconductors; J. Rice, S Lorentz, R. Datla, L. Vale, D Rudman, M. Lam Chok Sing, D. Robbes; Metrologia 1998, 35, 289 - 293